SCIENCE CHINA
Information Sciences

• REVIEW •

June 2025, Vol. 68, Iss. 6, 161201:1–161201:31
https://doi.org/10.1007/s11432-024-4437-9

An overview of recent advances in event-triggered control

Xian-Ming ZHANG[1], Qing-Long HAN[1*], Xiaohua GE[1], Derui DING[1], Boda NING[2] & Bao-Lin ZHANG[3]

[1] *School of Engineering, Swinburne University of Technology, Melbourne VIC 3122, Australia*
[2] *Department of Electrical and Electronic Engineering, Auckland University of Technology, Auckland 1010, New Zealand*
[3] *College of Automation and Electronic Engineering, Qingdao University of Science & Technology, Qingdao 266061, China*

Received 5 October 2024/Revised 7 February 2025/Accepted 21 March 2025/Published online 26 May 2025

Abstract Event-triggered control (ETC) offers an efficient strategy for significantly reducing communication and computation resources in networked systems by triggering control updates only when necessary. This study provides an overview of recent advances in ETC. First, data-driven (or model-free) ETC, which has gained significant attention in recent years, is reviewed for linear systems with and without unknown disturbances. Second, co-design issues are deeply analyzed for both state feedback and dynamic output feedback control. Third, the separation principle is thoroughly examined in the context of event-triggered observer-based output feedback control. Fourth, some insightful discussions are made on the ideal execution property of event-triggered schemes, as well as the modeling of ETC under packet dropouts. Finally, several challenging issues for future research are outlined.

Keywords event-triggered control, data-driven control, observer-based output feedback control, separation principle, Zeno behavior

Citation Zhang X-M, Han Q-L, Ge X H, et al. An overview of recent advances in event-triggered control. Sci China Inf Sci, 2025, 68(6): 161201, https://doi.org/10.1007/s11432-024-4437-9

1 Introduction

Event-triggered control (ETC) has emerged as a significant paradigm in networked systems. It aims to improve the efficiency of resource usage, such as communication bandwidth and computational power, by transmitting necessary data or executing control actions only when certain predefined conditions are violated, rather than at fixed periodic intervals. Up to date, ETC has been extensively applied in various areas, such as multi-agent systems, cyber-physical systems, and networked systems [1–14].

In [15], the idea of ETC is used to investigate the temporal properties of distributed real-time systems. A processing activity is initiated in two different ways: time-triggered, occurring periodically at predetermined points in time, and event-triggered, activated by the occurrence of a significant event. Detailed comparisons between event-triggered and time-triggered distributed real-time systems are made, focusing on various aspects such as predictability, testability, resource utilization, and extensibility. Similar results can also be found in [16] for distributed fault-tolerant real-time systems.

Experimental analysis of first-order stochastic systems revealed that event-triggered sampling produces substantially smaller variances for the same average sampling rate, providing better performance than periodic sampling. However, systems with event-triggered sampling are much harder to analyze than those with periodic sampling due to the time-varying nature of the closed-loop system [17]. To address this challenge, a state-dependent event-triggered scheduler was proposed in [18] to determine which control task to execute while guaranteeing the desired system performance.

The significance of the work [18] lies in its provision of a remarkable solution to event-triggered control from both implementation and theoretical analysis perspectives. Specifically, real-time scheduling for event-triggered execution can be easily implemented while ensuring the input-to-state stability of the closed-loop system. ETC has gained increasing attention in networked systems due to that it paves a

* Corresponding author (email: qhan@swin.edu.au)

new way to save limited communication and computation resources, as well as to prolong the lifespan of battery-based devices in networked systems. Therefore, a large number of results related to ETC have been published in the literature, e.g., [19–34].

One critical issue in ETC is that the minimum inter-event time between any two consecutive events should be strictly positive to exclude the so-called Zeno behavior [18]. Moreover, it has been noted that Zeno's behavior is possible even though sufficiently small disturbances are imposed on a system [35]. To address this issue, several event-triggered schemes have been proposed for systems with or without external disturbances. These include self-triggered schemes, mixed event-triggered schemes, periodic event-triggered schemes, dynamic event-triggered schemes, and adaptive event-triggered schemes. Based on these schemes, many useful models for event-triggered control systems have been proposed for stability analysis and control synthesis, e.g., [2, 6, 36–40].

Another concern in ETC is the co-design of both control gains and event-triggered parameters. Early results on ETC are based on the so-called emulation method. In this approach, the control gain is first designed in the continuous-time domain, where no signal sampling is involved. Then, proper event-triggered parameters are designed such that the controller ensures suitable control performance for the system under an event-triggered sampling scheme. Clearly, such a controller is independent of sampling. With this in mind, an event-triggered transmission scheme is proposed [41, 42], in which system signals are sampled periodically, and the decision to release the current sampled signal to the communication network is determined by a predefined event-triggered condition. This event-triggered transmission scheme not only excludes Zeno behavior but also allows for the co-design of both control gains and event-triggered parameters. For details, see [43].

Although significant progress has been made, several research gaps remain in ETC. Notable challenges include developing robust model-free or data-driven ETC approaches leveraging reinforcement learning or adaptive control, establishing rigorous stability guarantees for nonlinear and stochastic systems under event-triggered settings, designing integrated co-design strategies that optimize event-triggering conditions and control laws simultaneously, and developing ETC schemes resilient to network uncertainties while ensuring stability and performance. Consequently, ETC has remained a highly active research area in networked control over the past several years, with a primary focus on the following issues.

- Data-driven ETC. Data-driven ETC, also known as model-free ETC, has emerged as a promising approach to networked systems, where the underlying model is unknown or difficult to obtain. Unlike traditional model-based control methods that rely on accurate system models, data-driven ETC leverages real-time data to make control decisions, enabling more flexible and adaptable control strategies.
- Co-design of both the control law and the event-triggered sampling scheme. Traditional ETC typically follows an emulation-based approach, where the controller is designed without accounting for the properties of event-triggered sampling. Thus, it becomes significant to jointly design the control law and the event-triggered sampling scheme such that control performance and communication efficiency can be optimized simultaneously.
- Event-triggered observer-based output feedback control. In observer-based output feedback control, the separation principle asserts that the observer and controller can be designed independently, while still ensuring overall system stability. This simplifies the design process by allowing the observer and control law to be developed separately. However, when introducing an event-triggered scheme, whether the separation principle remains valid requires further investigation.
- Some other issues about the ideal execution property of an event-triggered scheme and ETC under packet dropouts. Recent research has shown that several event-triggered schemes exhibit the ideal execution property, meaning they remain inactive during exponentially stable trajectories. Such schemes trigger the minimum number of events necessary to maintain the system's exponential stability. On the other hand, increasing attention has been directed toward ETC under packet dropouts. It is indicated that an ETC system subject to packet dropouts can be modeled as a hybrid system by introducing proper auxiliary variables.

This study provides a comprehensive overview of recent developments in ETC, offering valuable insights into key issues above. First, data-driven ETC for linear systems, both with and without unknown disturbances, is examined in detail under static and dynamic event-triggered schemes. Second, significant advances in the joint design of control laws and event-triggering mechanisms are thoroughly explored for (disturbed) linear systems. Third, the separation principle in the context of event-triggered observer-based output feedback control is reviewed. Then, considerable attention is paid to critical topics such as the ideal execution property of event-triggered schemes and ETC in the presence of packet dropouts.

Finally, several key challenges and directions for future research are highlighted.

Notations. diag$\{\cdots\}$ and col$\{\cdots\}$ denote a block-diagonal matrix and a block-column matrix (vector), respectively. The symbol '$\star$' in a symmetric block matrix stands for a term induced by symmetry. $\mathbb{Z}_{\geqslant 0}$ means the set of non-negative integers. $\mathcal{L}_2\,[t_0,\infty)$ denotes the space of square-integrable vector functions over $[t_0,\infty)$. $\mathrm{He}\{A\}=A+A^{\mathrm{T}}$, where X^{T} is the transpose of X. $\lambda_{\min}(A)$ ($\lambda_{\max}(A)$) means the minimum (maximum) eigenvalue of the symmetric matrix A. $A^{\dagger}$ denotes the Moore-Penrose inverse of A.

2 Event-triggered control from data

Usually, in traditional ETC, both control gains and event-triggering conditions are designed based on system models. When system models are not available, control gains and event-triggering conditions can be obtained based on input-state/output data from experiments, leading to data-driven ETC [44–46].

2.1 Data-driven ETC for unforced linear systems

Consider the following unforced continuous-time system:

$$\dot{x}(t)=Ax(t)+Bu(t), \tag{1}$$

where $x(t)\in\mathbb{R}^n$ and $u(t)\in\mathbb{R}^m$ are the state vector and the control input, respectively. $A\in\mathbb{R}^{n\times n}$ and $B\in\mathbb{R}^{n\times m}$ are constants but unknown. By the emulation method, one first designs a controller $u(t)=Kx(t)$ to ensure that the closed-loop system (1) without sampling meets a certain performance criterion. Subsequently, an event-triggered mechanism is designed so that the resultant ETC system maintains this performance.

Since A and B are unknown, we need a set of data collected offline, given by

$$\mathbb{D}=\{u(iT_s),x(iT_s),\dot{x}(iT_s)\big|i=0,1,2,\ldots,L-1\}, \tag{2}$$

where T_s is the sampling period in an experiment for data collection and L is the number of samples. From these data, let

$$\begin{aligned}U_0&=\big[u(0)\ u(T_s)\ u(2T_s)\ \cdots\ u((L-1)T_s)\big],\\X_0&=\big[x(0)\ x(T_s)\ x(2T_s)\ \cdots\ x((L-1)T_s)\big],\\X_1&=\big[\dot{x}(0)\ \dot{x}(T_s)\ \dot{x}(2T_s)\ \cdots\ \dot{x}((L-1)T_s)\big].\end{aligned}$$

Then it is not difficult to verify that

$$X_1=AX_0+BU_0=[B\ A]\begin{bmatrix}U_0\\X_0\end{bmatrix}. \tag{3}$$

One of critical questions is how much data are needed from experiments for the data-driven ETC. The following crucial assumption gives an answer to the question.

Assumption 1. The matrix col$\{U_0,X_0\}$ has full row rank $n+m$.

By Willem's lemma for continuous-time systems [47], if the input u is persistently exciting of order $n+1$, then Assumption 1 is satisfied. In this way, it is not difficult to have $L\geqslant(n+1)m+n$, which means that one needs at least $(n+1)m+n$ data for data-driven ETC.

Under Assumption 1, one can design parameterized state feedback controllers in advance and then design suitable event-triggering conditions to save communication resources when control signals are transmitted.

2.1.1 *Control design from data*

The objective of control design from data is to design a control gain K such that the matrix $A+BK$ is Hurwitz. Under Assumption 1, the matrix col$\{U_0,X_0\}$ has full row rank. Thus, there exists a matrix $G\in\mathbb{R}^{L\times n}$ such that

$$\begin{bmatrix}K\\I\end{bmatrix}=\begin{bmatrix}U_0\\X_0\end{bmatrix}G \tag{4}$$

which, together with (3), leads to the following data-based representation of the matrix $A+BK$:

$$A+BK=[B\ A]\begin{bmatrix}K\\I\end{bmatrix}=[B\ A]\begin{bmatrix}U_0\\X_0\end{bmatrix}G=X_1G. \tag{5}$$

Thus, by employing the Lyapunov theorem, the matrix $A+BK$ is Hurwitz if and only if there exists a positive-definite matrix P such that $X_1GP+P(X_1G)^{\mathrm{T}}<0$. Let $Q=GP$. Then from (3), $KP=U_0GP=U_0Q$ and $P=X_0GP=X_0Q$. Thus, one can conclude that the control gain $K=U_0Q(X_0Q)^{-1}$ renders the matrix $A+BK$ Hurwitz if the following linear matrix inequalities (LMIs) on the matrix variable Q are satisfied:

$$X_1Q+Q^{\mathrm{T}}X_1^{\mathrm{T}}<0,\quad X_0Q>0. \tag{6}$$

From the analysis above, under Assumption 1, all parameterized controller gains such that $A+BK$ is Hurwitz are designed in terms of data-based LMIs. If the data-based LMIs in (6) are feasible, the closed-loop system of (1) with $u(t)=Kx(t)$ is globally exponentially stable.

2.1.2 *Event-triggering conditions from data*

Let Q satisfy (6). Data-driven ETC is to design an ETC policy to sample system signals such that the closed-loop system with $K=U_0Q(X_0Q)^{-1}$ preserves global exponential stability. Similar to [18], the ETC can be predefined as

$$t_{k+1}=\inf\left\{t>t_k|e^{\mathrm{T}}(t)\Omega e(t)>\sigma x^{\mathrm{T}}(t)\Omega x(t)\right\}, \tag{7}$$

where $e(t)=x(t)-x(t_k)$, $\sigma>0$ is a threshold, and $\Omega>0$ is a weighted matrix. The introduction of Ω makes the ETC (7) more general. There may be an intrinsic relationship between Ω and σ. To uncover this relationship, one typically establishes stability criteria that depend on both σ and Ω. Based on these criteria, the weighted matrix Ω can be designed for a given σ, or alternatively, the threshold σ can be determined by setting $\Omega=I$.

Under the ETC (7), the closed-loop ETC system of (1) can be given by

$$\dot{x}(t)=(A+BK)x(t)+BKe(t),\ t\in[t_k,t_{k+1}). \tag{8}$$

Theorem 1. Under Assumption 1, consider the system (8) with $K=U_0Q(X_0Q)^{-1}$, where Q satisfies (6). For given $\sigma>0$ and a real matrix $H\in\mathbb{R}^{L\times n}$ such that

$$\begin{bmatrix}K\\0\end{bmatrix}=\begin{bmatrix}U_0\\X_0\end{bmatrix}H, \tag{9}$$

the closed-loop system (8) remains globally exponentially stable if there exists a matrix $\tilde{\Omega}>0$ such that

$$\begin{bmatrix}X_1Q+Q^{\mathrm{T}}X_1^{\mathrm{T}}+\sigma\tilde{\Omega} & X_1HX_0Q\\ \star & -\tilde{\Omega}\end{bmatrix}<0. \tag{10}$$

Moreover, the weighted matrix Ω can be designed as $\Omega=(X_0Q)^{-1}\tilde{\Omega}(X_0Q)^{-1}$.

Proof. Choose a Lyapunov function $V=x^{\mathrm{T}}P^{-1}x$ with $P=X_0Q$. Then

$$\dot{V}(t)|_{(8)}=\begin{bmatrix}x(t)\\e(t)\end{bmatrix}^{\mathrm{T}}\begin{bmatrix}P^{-1}(A+BK)+(A+BK)^{\mathrm{T}}P^{-1} & P^{-1}BK\\ \star & 0\end{bmatrix}\begin{bmatrix}x(t)\\e(t)\end{bmatrix}. \tag{11}$$

From (7), for $t\in[t_k,t_{k+1})$, $e^{\mathrm{T}}(t)\Omega e(t)\leqslant\sigma x^{\mathrm{T}}(t)\Omega x(t)$. Thus, it follows from (11) that

$$\dot{V}(t)|_{(8)}\leqslant\begin{bmatrix}x(t)\\e(t)\end{bmatrix}^{\mathrm{T}}\begin{bmatrix}P^{-1}(A+BK)+(A+BK)^{\mathrm{T}}P^{-1}+\sigma\Omega & P^{-1}BK\\ \star & -\Omega\end{bmatrix}\begin{bmatrix}x(t)\\e(t)\end{bmatrix}. \tag{12}$$

We now prove that Eq. (10) ensures

$$\begin{bmatrix} P^{-1}(A+BK)+(A+BK)^{\mathrm{T}}P^{-1}+\sigma\Omega & P^{-1}BK \\ \star & -\Omega \end{bmatrix} < 0 \tag{13}$$

$$\Longleftrightarrow \begin{bmatrix} (A+BK)P+P(A+BK)^{\mathrm{T}}+\sigma\tilde{\Omega} & BKP \\ \star & -\tilde{\Omega} \end{bmatrix} < 0, \tag{14}$$

where $\tilde{\Omega} = P\Omega P$. In fact, from (5) and (9), $A+BK = X_1G$ and

$$BK = [B\ A]\begin{bmatrix} K \\ 0 \end{bmatrix} = [B\ A]\begin{bmatrix} U_0 \\ X_0 \end{bmatrix} H = X_1H.$$

Substituting $A+BK = X_1G$ and $BK = X_1H$ into (14), together with $GP = Q$ and $P = X_0Q$, yields (10).

Theorem 1 provides a data-based LMI method to design a suitable event-triggered parameter Ω for a given threshold $\sigma > 0$. If setting the weighted matrix $\Omega = I$, Theorem 1 can be used to design the threshold parameter σ, which means that a suitable data-driven ETC can be devised based on data collected from experiments.

Another interesting result is that the data-driven ETC (7) offers a global minimum inter-event time.

Theorem 2. Under Assumption 1, if the data-driven ETC (7) renders the closed-loop system (8) to remain globally exponentially stable, then the inter-event time $t_{k+1} - t_k$ satisfies

$$t_{k+1} - t_k \geqslant \frac{1}{c_0}\frac{\sqrt{\sigma}}{1+\sqrt{\sigma}}, \quad k = 0, 1, 2, \ldots \tag{15}$$

Proof. Let $\|\Omega^{\frac{1}{2}}x(t)\| = \sqrt{x^{\mathrm{T}}(t)\Omega x(t)}$. Then

$$\begin{aligned} \frac{\mathrm{d}}{\mathrm{d}t}\frac{\|\Omega^{\frac{1}{2}}e(t)\|}{\|\Omega^{\frac{1}{2}}x(t)\|} &= \frac{e^{\mathrm{T}}(t)\Omega\dot{e}(t)}{\|\Omega^{\frac{1}{2}}e(t)\|\|\Omega^{\frac{1}{2}}x(t)\|} - \frac{\|\Omega^{\frac{1}{2}}e(t)\|x^{\mathrm{T}}(t)\Omega\dot{x}(t)}{\|\Omega^{\frac{1}{2}}x(t)\|^3} \\ &\leqslant \frac{\|\Omega^{\frac{1}{2}}\dot{x}(t)\|}{\|\Omega^{\frac{1}{2}}x(t)\|} + \frac{\|\Omega^{\frac{1}{2}}e(t)\|\|\Omega^{\frac{1}{2}}\dot{x}(t)\|}{\|\Omega^{\frac{1}{2}}x(t)\|^2} \\ &= \left(1+\frac{\|\Omega^{\frac{1}{2}}e(t)\|}{\|\Omega^{\frac{1}{2}}x(t)\|}\right)\frac{\|\Omega^{\frac{1}{2}}\dot{x}(t)\|}{\|\Omega^{\frac{1}{2}}x(t)\|}. \end{aligned} \tag{16}$$

Note that from (8), $\dot{x}(t) = X_1Gx(t) + X_1He(t)$, which leads to

$$\frac{\|\Omega^{\frac{1}{2}}\dot{x}(t)\|}{\|\Omega^{\frac{1}{2}}x(t)\|} \leqslant c_0\left(1+\frac{\|\Omega^{\frac{1}{2}}e(t)\|}{\|\Omega^{\frac{1}{2}}x(t)\|}\right), \tag{17}$$

where $c_0 = \max\left\{\|\Omega^{\frac{1}{2}}X_1G\Omega^{-\frac{1}{2}}\|, \|\Omega^{\frac{1}{2}}X_1H\Omega^{-\frac{1}{2}}\|\right\}$. Combining (16) and (17) gives

$$\frac{\mathrm{d}}{\mathrm{d}t}\frac{\|\Omega^{\frac{1}{2}}e(t)\|}{\|\Omega^{\frac{1}{2}}x(t)\|} \leqslant c_0\left(1+\frac{\|\Omega^{\frac{1}{2}}e(t)\|}{\|\Omega^{\frac{1}{2}}x(t)\|}\right)^2. \tag{18}$$

Consider the differential inequality $\dot{\alpha} \leqslant c_0(1+\alpha)^2$ with initial condition $\alpha(t_k) = 0$. When α grows from 0 at t_k to $\sqrt{\sigma}$ at t_{k+1}, we readily obtain (15).

Theorem 2 shows that the data-driven ETC (7) has a global minimum inter-event time $\frac{\sqrt{\sigma}}{c_0(1+\sqrt{\sigma})}$, independent of system initial values, which is different from that for model-based ETC [18].

2.1.3 *Co-design from data*

The analysis above presents an emulation-based method to design ETC from data. A natural question raises: Is it possible to co-design both the control gain K and the ETC parameter Ω from data? In the following, we give some discussion on this question.

Based on the lines of the proof of Theorem 1, we need the inequality (14) to be satisfied. Substituting $A + BK = X_1 G$ and $BK = X_1 H$ into it yields

$$\begin{bmatrix} X_1 GP + PG^{\mathrm{T}} X_1^{\mathrm{T}} + \sigma\tilde{\Omega} & X_1 HP \\ \star & -\tilde{\Omega} \end{bmatrix} < 0. \tag{19}$$

Set $GP = Q_1$ and $HP = Q_2$. Then the inequality (19) becomes

$$\begin{bmatrix} X_1 Q_1 + Q_1^{\mathrm{T}} X_1^{\mathrm{T}} + \sigma\tilde{\Omega} & X_1 Q_2 \\ \star & -\tilde{\Omega} \end{bmatrix} < 0 \tag{20}$$

which seems a data-based LMI on the matrix variables $(Q_1, Q_2, \tilde{\Omega})$. However, inherited from (4) and (9), the matrix variables Q_1 and Q_2 should also satisfy

$$X_0 Q_1 > 0,\ U_0 Q_1 = U_0 Q_2,\ X_0 Q_2 = 0. \tag{21}$$

If the constraints (20) and (21) are satisfied, the control gain and the weighted matrix Ω can be given by $K = U_0 Q_1 (X_0 Q_1)^{-1}$ and $\Omega = (X_0 Q_1)^{-1} \tilde{\Omega} (X_0 Q_1)^{-1}$. Thus, we have the following result.

Theorem 3. Under Assumption 1, for a certain threshold $\sigma > 0$, the data-driven ETC (7) with $\Omega = (X_0 Q_1)^{-1} \tilde{\Omega} (X_0 Q_1)^{-1}$ can ensure that the closed-loop system (8) with $K = U_0 Q_1 (X_0 Q_1)^{-1}$ is globally exponentially stable if there exist real matrix $\tilde{\Omega} > 0$, Q_1, Q_2 with $Q_1 - Q_2 \in \ker\{U_0\}$ and $Q_2 \in \ker\{X_0\}$ such that the LMIs $X_0 Q_1 > 0$ and (20) are satisfied. Moreover, the minimum inter-event time is greater than $\frac{\sqrt{\sigma}}{c_0(1+\sqrt{\sigma})}$.

2.1.4 *Dynamic ETC from data*

The ETC (7) is static in the sense that it only involves the current value of x and e. Similar to [48], we consider the following dynamic ETC:

$$t_{k+1} = \inf\left\{t > t_k \middle|\ \eta(t) - \theta\left[e^{\mathrm{T}}(t)\Omega e(t) - \sigma x^{\mathrm{T}}(t)\Omega x(t)\right] \leqslant 0\right\}, \tag{22}$$

where $\theta \geqslant 0$ is a certain parameter and $\eta(t) \in \mathbb{R}_{\geqslant 0}$ is an internal variable, whose dynamic is given by

$$\dot{\eta}(t) = -\lambda\eta(t) - \left[e^{\mathrm{T}}(t)\Omega e(t) - \sigma x^{\mathrm{T}}(t)\Omega x(t)\right],\quad \eta(0) = \eta_0 \geqslant 0. \tag{23}$$

Clearly, η can be regarded as a filtered value of $\sigma x^{\mathrm{T}}(t)\Omega x(t) - e^{\mathrm{T}}(t)\Omega e(t)$ [48]. In this sense, we call it a dynamic ETC, under which the closed-loop system augmented by (8) and (23) is given by

$$\begin{cases} \dot{x}(t) = (A + BK)x(t) + BKe(t), \\ \dot{\eta}(t) = -\lambda\eta(t) - \left[e^{\mathrm{T}}(t)\Omega e(t) - \sigma x^{\mathrm{T}}(t)\Omega x(t)\right], \\ (x(0), \eta(0)) = (x_0, \eta_0). \end{cases} \tag{24}$$

If taking a Lyapunov function

$$\widetilde{V}(t) = x^{\mathrm{T}}(t) P^{-1} x(t) + \eta,\quad P = X_0 Q, \tag{25}$$

then Theorems 1–3 above remain true for the augmented system (24) under the dynamic ETC (22). The difference is that, under the dynamic ETC (22), the inter-event time can be enlarged by tuning the parameter θ as done in [48].

2.2 Data-driven ETC for linear systems with unknown noisy

Consider the system with disturbance

$$\dot{x}(t) = Ax(t) + Bu(t) + d(t), \tag{26}$$

where $d(t) \in \mathbb{R}^n$ is unknown. Since the existence of unknown disturbance in the system, the data collected from experiments are thus noised, complicating the exact data-based representation of the closed-loop system. Moreover, the noisy data also make Zeno behavior possible. In the following, we present an emulation-based method to design data-driven ETCs from data. For this goal, let

$$D_0 = \left[d(0)\ d(T_s)\ d(2T_s)\ \cdots\ d((L-1)T_s)\right].$$

Then from (26), one has $X_1 = AX_0 + BU_0 + D_0$.

2.2.1 *Control design from data*

Due to the unknown $d(t)$, the data D_0 are also unknown. Without loss of generality, suppose that there exists a real matrix F such that $D_0 D_0^{\mathrm{T}} \leqslant FF^{\mathrm{T}}$. Under this assumption, we now design a state feedback control $u = Kx$ from data such that the closed-loop system $\dot{x}(t) = (A + BK)x(t) + d(t)$ is ISS with respect to the disturbance input $d(t)$.

From (4), together with $X_1 = AX_0 + BU_0 + D_0$, one has

$$A + BK = [B \ A] \begin{bmatrix} K \\ I \end{bmatrix} = [B \ A] \begin{bmatrix} U_0 \\ X_0 \end{bmatrix} G = (X_1 - D_0)G. \tag{27}$$

On the other hand, it is easy to draw a conclusion that the system $\dot{x}(t) = (A + BK)x(t) + d(t)$ is ISS with respect to $d(t)$ if there exist real matrices $P > 0$ and $S > 0$ such that

$$(A + BK)P + P(A + BK)^{\mathrm{T}} + S < 0. \tag{28}$$

Due to unknown matrices A and B, substituting (27) into (28) and letting $Q = GP$, the matrix inequality (28) becomes

$$X_1 Q + Q^{\mathrm{T}} X_1^{\mathrm{T}} - D_0 Q - Q^{\mathrm{T}} D_0^{\mathrm{T}} + S < 0. \tag{29}$$

Note that $-D_0 Q - Q^{\mathrm{T}} D_0^{\mathrm{T}} \leqslant \varepsilon D_0 D_0^{\mathrm{T}} + \varepsilon^{-1} Q^{\mathrm{T}} Q \leqslant \varepsilon FF^{\mathrm{T}} + \varepsilon^{-1} Q^{\mathrm{T}} Q$ for any scalar $\varepsilon > 0$. Thus, the inequality (29) can be ensured if the following data-based LMI holds:

$$\begin{bmatrix} X_1 Q + Q^{\mathrm{T}} X_1^{\mathrm{T}} + \varepsilon FF^{\mathrm{T}} + S & Q^{\mathrm{T}} \\ \star & -\varepsilon I \end{bmatrix} < 0. \tag{30}$$

Moreover, from (4), it is clear that $P = X_0 Q$ and $KP = U_0 Q$. Therefore, if there exist real matrices Q and $S > 0$, and a scalar $\varepsilon > 0$ such that (30) and $X_0 Q > 0$, then the control gain $K = U_0 Q (X_0 Q)^{-1}$ can render the system $\dot{x}(t) = (A + BK)x(t) + d(t)$ ISS with respect to $d(t)$.

2.2.2 *Event-triggering conditions design from data*

We still consider the data-driven ETC (7). Then under the control of $u = Kx$ with $K = U_0 Q (X_0 Q)^{-1}$, the event-triggered closed-loop system of (26) reads as

$$\dot{x}(t) = (A + BK)x(t) + BKe(t) + d(t), \quad t \in [t_k, t_{k+1}). \tag{31}$$

Now, we are to design a suitable weighted matrix $\Omega > 0$ for a proper threshold $\sigma > 0$ such that the predesigned controller can preserve the system (31) to be ISS with respect to $d(t)$.

Theorem 4. Under Assumption 1 and $D_0 D_0^{\mathrm{T}} \leqslant FF^{\mathrm{T}}$, for a proper threshold $\sigma > 0$, the closed-loop system (31) with $K = U_0 Q (X_0 Q)^{-1}$ is ISS with respect to $d(t)$ if there exist two real matrices $\tilde{\Omega} > 0$, $S > 0$ and a scalar $\varepsilon > 0$ such that

$$\begin{bmatrix} X_1 Q + (X_1 Q)^{\mathrm{T}} + \sigma \tilde{\Omega} + S + \varepsilon FF^{\mathrm{T}} & X_1 H X_0 Q & Q^{\mathrm{T}} \\ \star & -\tilde{\Omega} & (HX_0 Q)^{\mathrm{T}} \\ \star & \star & -\varepsilon I \end{bmatrix} < 0. \tag{32}$$

Moreover, the weighted matrix Ω in (7) can be designed as $\Omega = (X_0 Q)^{-1} \tilde{\Omega} (X_0 Q)^{-1}$.

Proof. Let $V(t) = x^{\mathrm{T}}(t) P^{-1} x(t)$ with $P = X_0 Q$. Then, for $t \in [t_k, t_{k+1})$,

$$\begin{aligned} \frac{\mathrm{d}}{\mathrm{d}t} V(t)|_{(31)} &= 2x^{\mathrm{T}}(t) P^{-1} \big[(A + BK)x(t) + BKe(t) + d(t)\big] \\ &\leqslant 2x^{\mathrm{T}}(t) P^{-1} \big[(A + BK)x(t) + BKe(t)\big] + x^{\mathrm{T}}(t) P^{-1} S P^{-1} x(t) + d^{\mathrm{T}}(t) S^{-1} d(t) \\ &\quad + \sigma x^{\mathrm{T}}(t) \Omega x(t) - e^{\mathrm{T}}(t) \Omega e(t) \end{aligned}$$

$$= \begin{bmatrix} P^{-1}x(t) \\ P^{-1}e(t) \end{bmatrix}^{\mathrm{T}} \begin{bmatrix} (A+BK)P+P(A+BK)^{\mathrm{T}}+\sigma\tilde{\Omega}+S & BKP \\ \star & -\tilde{\Omega} \end{bmatrix} \begin{bmatrix} P^{-1}x(t) \\ P^{-1}e(t) \end{bmatrix} + d^{\mathrm{T}}(t)S^{-1}d(t), \tag{33}$$

where $S > 0$ and $\tilde{\Omega} = P\Omega P$. Thus, it is concluded that the system (31) is ISS with respect to $d(t)$ if the following inequality holds:

$$\begin{bmatrix} (A+BK)P + P(A+BK)^{\mathrm{T}} + \sigma\tilde{\Omega} + S & BKP \\ \star & -\tilde{\Omega} \end{bmatrix} < 0. \tag{34}$$

Substituting $A + BK = (X_1 - D_0)G$, $BK = (X_1 - D_0)H$, $GP = Q$, and $P = X_0Q$ into (34) yields

$$\Phi \triangleq \begin{bmatrix} (X_1 - D_0)Q + [(X_1 - D_0)Q]^{\mathrm{T}} + \sigma\tilde{\Omega} + S & (X_1 - D_0)HX_0Q \\ \star & -\tilde{\Omega} \end{bmatrix} < 0. \tag{35}$$

Note that

$$\begin{aligned} \Phi &= \begin{bmatrix} X_1Q+(X_1Q)^{\mathrm{T}}+\sigma\tilde{\Omega}+S & X_1HX_0Q \\ \star & -\tilde{\Omega} \end{bmatrix} + \begin{bmatrix} -I \\ 0 \end{bmatrix} D_0 \begin{bmatrix} Q & HX_0Q \end{bmatrix} + \begin{bmatrix} Q^{\mathrm{T}} \\ (HX_0Q)^{\mathrm{T}} \end{bmatrix} D_0^{\mathrm{T}} \begin{bmatrix} -I & 0 \end{bmatrix} \\ &\leqslant \begin{bmatrix} X_1Q+(X_1Q)^{\mathrm{T}}+\sigma\tilde{\Omega}+S & X_1HX_0Q \\ \star & -\tilde{\Omega} \end{bmatrix} + \varepsilon \begin{bmatrix} -I \\ 0 \end{bmatrix} D_0D_0^{\mathrm{T}} \begin{bmatrix} -I \\ 0 \end{bmatrix}^{\mathrm{T}} + \varepsilon^{-1} \begin{bmatrix} Q^{\mathrm{T}} \\ (HX_0Q)^{\mathrm{T}} \end{bmatrix} \begin{bmatrix} Q^{\mathrm{T}} \\ (HX_0Q)^{\mathrm{T}} \end{bmatrix}^{\mathrm{T}}, \end{aligned} \tag{36}$$

where $\varepsilon > 0$. Thus $\Phi < 0$ for $D_0D_0^{\mathrm{T}} \leqslant FF^{\mathrm{T}}$ is implied by

$$\begin{bmatrix} X_1Q+(X_1Q)^{\mathrm{T}}+\sigma\tilde{\Omega}+S & X_1HX_0Q \\ \star & -\tilde{\Omega} \end{bmatrix} + \varepsilon \begin{bmatrix} -I \\ 0 \end{bmatrix} FF^{\mathrm{T}} \begin{bmatrix} -I \\ 0 \end{bmatrix}^{\mathrm{T}} + \varepsilon^{-1} \begin{bmatrix} Q^{\mathrm{T}} \\ (HX_0Q)^{\mathrm{T}} \end{bmatrix} \begin{bmatrix} Q^{\mathrm{T}} \\ (HX_0Q)^{\mathrm{T}} \end{bmatrix}^{\mathrm{T}} < 0 \tag{37}$$

which is equivalent to (32) using the Schur complement.

Theorem 4 provides a data-based LMI algorithm to devise a suitable ETC for a proper threshold σ. If setting $\Omega = I$, then one can derive a suitable threshold σ from Theorem 4 using off-line data, ensuring that the closed-loop system (31) remains ISS with respect to the disturbance input $d(t)$. However, due to the presence of $d(t)$, even it is arbitrarily small, the ETC (7) cannot guarantee that the minimum inter-event time $\min\{t_{k+1} - t_k | k \in \mathbb{Z}_{\geqslant 0}\}$ is positive, implying that Zeno behavior is possible [46].

In order to exclude Zeno's behavior, two approaches are proposed in [46]. The first approach weakens the ISS property to practical stability, ensuring that the solution to (31) satisfies $\|x(t)\| \leqslant c_0e^{-c_1t}\|x_0\| + c_2\|d(t)\|_{[0,t]} + c_3\mu$, where $c_0 \geqslant 1$, $c_i > 0$ $(i = 1, 2, 3)$ and $\mu > 0$ is a tuning parameter. The ETC (7) is then modified as

$$t_{k+1} = \inf\left\{t > t_k \;\middle|\; e^{\mathrm{T}}(t)\Omega e(t) > \sigma x^{\mathrm{T}}(t)\Omega x(t) + \mu\right\}. \tag{38}$$

The second approach changes the ETC (7) to a time-regulated ETC:

$$t_{k+1} = \inf\left\{t > t_k + \tau(\sigma) \;\middle|\; e^{\mathrm{T}}(t)\Omega e(t) > \sigma x^{\mathrm{T}}(t)\Omega x(t)\right\}, \tag{39}$$

where $\tau(\sigma) > 0$ is a time-regulated parameter.

Similar to the proof of Theorem 2, the data-driven ETC (38) ensures a global minimum inter-event time for the practical stability of the closed-loop system (31). By choosing a small positive number τ_0 such that $\tau(\sigma) \geqslant \tau_0 > 0$, the data-driven ETC (39) can not only exclude Zeno behavior but also ensure the closed-loop system (31) achieves the ISS property rather than just practical stability.

Theorem 4 remains valid if the static ETC (7) is replaced with the dynamic ETC (22). Similar to the previous discussion, under the conditions in Theorem 4, the dynamic ETC cannot exclude Zeno behavior. To address this, a modified dynamic ETC is proposed in [46] by weakening the system performance. It remains challenging to design a data-based dynamic ETC for the noisy system (26) that ensures both a global minimum inter-event time and improved performance. This section focuses on data-driven ETC for continuous-time linear systems. For the corresponding methods applicable to discrete-time systems, please refer to [44, 45, 49, 50].

In recent years, data-driven control (DDC) has regained increasing attention, particularly following the work [51], where a parametrization of linear feedback systems is derived based on Willems et al's fundamental lemma [52]. The key idea is the data-based representations in (3) and (5), from which the open-loop system can be expressed as $\dot{x}(t) = X_1 \left[\begin{smallmatrix} U_0 \\ X_0 \end{smallmatrix}\right]^{\dagger} \left[\begin{smallmatrix} u(t) \\ x(t) \end{smallmatrix}\right]$, and the closed-loop system as $\dot{x}(t) = X_1 G x(t)$. This method needs to know the dimensions of system state and input while assuming the coefficient matrices A and B are unknown. These characteristics prevent it being a 'genuine' DDC strategy. A true DDC approach does not require an explicit mathematical model, instead leveraging historical or real-time data to infer system dynamics, leading to notable approaches, such as reinforcement learning, adaptive control, and machine learning-based optimization [53]. Integrating event-triggered schemes into these DDC approaches remains a research challenge that requires further investigation.

3 Co-design of both event-triggered sampling schemes and control gains

Traditional ETC methods typically follow an emulation approach. Initially, an appropriate control law is designed in continuous time, and then an event-triggered sampling scheme is developed to ensure that the sampled-data system performs as closely as possible to its continuous-time counterpart. However, this approach often overlooks the practical aspects of implementing the sampling scheme and network constraints. In recent years, considerable efforts have been made to address this co-design challenge, as reviewed briefly in what follows.

3.1 Linear systems without external disturbances

Consider the following unforced linear system:

$$\dot{x}(t) = Ax(t) + Bu(t), \quad x(t_0) = x_0, \tag{40}$$

where $x \in \mathbb{R}^n, u \in \mathbb{R}^m$ are the system state and input vector, and the matrices $A \in \mathbb{R}^{n\times n}$ and $B \in \mathbb{R}^{n\times m}$ are known. Now, we consider the problem of co-design for the system (40), to design both an event-triggered scheme and a proper control gain such that (i) Zeno behavior is excluded; and (ii) the closed-loop system is asymptotically stable.

The co-design problem above for the system (40) is not difficult to cope with. Suppose $u(t) = Kx(t)$ with K being the control gain to be designed. Consider the event-triggered scheme in which the event time sequence $\{t_{k+1} | k = 0, 1, 2, \ldots\}$ is determined by

$$t_{k+1} = \inf\{t > t_k \mid e^{\mathrm{T}}(t)\Omega e(t) > \sigma x^{\mathrm{T}}(t)\Omega x(t)\}, \quad e(t) = x(t) - x(t_k), \tag{41}$$

where $\Omega > 0$ is a weighted matrix and $\sigma > 0$ is a threshold. It is clear from [18] that the event-triggered scheme (41) can ensure a positive minimum inter-event time. Thus, to address the co-design issue, we only need to present an algorithm to design Ω and K such that the resultant closed-loop system

$$\dot{x}(t) = (A + BK)x(t) + BKe(t), \quad x(t_0) = x_0 \tag{42}$$

is asymptotically stable. There are usually two approaches to get a criterion to design Ω and K for a certain threshold σ.

The first approach is to choose a Lyapunov function $V(t) = x^{\mathrm{T}}(t)P^{-1}x(t)$ with $P > 0$. Then, we have the following result.

Theorem 5. For given a scalar $\sigma > 0$, the closed-loop system (42) is asymptotically stable with $K = YP^{-1}$ if there exist positive-definite matrices P and $\tilde{\Omega}$ and a real matrix Y with appropriate dimensions such that

$$\begin{bmatrix} AP + BY + PA^{\mathrm{T}} + Y^{\mathrm{T}}B^{\mathrm{T}} + \sigma\tilde{\Omega} & BY \\ \star & -\tilde{\Omega} \end{bmatrix} < 0. \tag{43}$$

Moreover, the weighted matrix Ω in the ETC (41) is given as $\Omega = P^{-1}\tilde{\Omega}P^{-1}$.

Proof. Taking the derivative of $V(t)$ along with (42), together with the fact that $e^{\rm T}(t)\Omega e(t) \leqslant \sigma x^{\rm T}(t)\Omega x(t)$ for $t \in [t_k, t_{k+1})$, we have

$$\begin{aligned}\dot{V}(t) &= 2x^{\rm T}(t)P^{-1}[(A+BK)x(t)+BKe(t)],\ t\in[t_k,t_{k+1})\\ &\leqslant 2x^{\rm T}(t)P^{-1}[(A+BK)x(t)+BKe(t)]+\sigma x^{\rm T}(t)\Omega x(t)-e^{\rm T}(t)\Omega e(t)\\ &=\begin{bmatrix}P^{-1}x(t)\\P^{-1}e(t)\end{bmatrix}^{\rm T}\begin{bmatrix}(A+BK)P+P(A+BK)^{\rm T}+\sigma P\Omega P & BKP\\ \star & -P\Omega P\end{bmatrix}\begin{bmatrix}P^{-1}x(t)\\P^{-1}e(t)\end{bmatrix}.\end{aligned} \tag{44}$$

Let $Y = KP$ and $\tilde{\Omega} = P\Omega P$. Then the closed-loop system (42) is asymptotically stable if the linear matrix inequality (43) is satisfied.

The second approach is to follow the looped functional method. Let $L \in \mathbb{R}^{n\times n}$ be invertible and let $\tilde{x}(t) = L^{-1}x(t)$ and $\tilde{e}(t) = \tilde{x}(t) - \tilde{x}(t_k)$. Choose a functional as, e.g., [54]

$$\mathcal{W}(t) = \tilde{x}^{\rm T}(t)P\tilde{x}(t) + \mathcal{V}_0(t), \tag{45}$$

$$\mathcal{V}_0(t) = (t_{k+1}-t)\left\{\tilde{e}^{\rm T}(t)[S_1\tilde{e}(t)+2S_2\tilde{x}(t_k)] + (t-t_k)\tilde{x}^{\rm T}(t_k)S_3\tilde{x}(t_k) + \int_{t_k}^{t}\dot{\tilde{x}}^{\rm T}(s)R\dot{\tilde{x}}(s){\rm d}s\right\}, \tag{46}$$

where $\mathcal{V}_0(t)$ is a looped functional due to $\mathcal{V}_0(t_k) = \mathcal{V}_0(t_{k+1}) = 0$. To move on, let $T_k = t_{k+1} - t_k$ ($k = 0, 1, 2, \ldots$) and suppose that there exist two positive numbers $T_{\min}$ and $T_{\max}$ such that $T_{\min} \leqslant T_k \leqslant T_{\max}$. Clearly, the existence of $T_{\min}$ is ensured by the ETC (41). Then, applying the looped functional method with (45), we have the following result.

Theorem 6. For given scalars $T_{\min}$, $T_{\max}$, and $\sigma > 0$, the closed-loop system (42) with $K = YL^{-1}$ is asymptotically stable if there exist positive-definite matrices $P, R, \tilde{\Omega}$ and real matrices S_1, S_2, S_3, L, M, and Y with compatible dimensions such that

$$\Phi_0 + T_{\min}\Phi_1 < 0,\ \Phi_0 + T_{\max}\Phi_1 < 0, \tag{47}$$

$$\begin{bmatrix}\Phi_0 - T_{\min}E_3^{\rm T}S_3E_3 & T_{\min}E_0^{\rm T}M^{\rm T}\\ \star & -T_{\min}R\end{bmatrix} < 0,\ \begin{bmatrix}\Phi_0 - T_{\max}E_3^{\rm T}S_3E_3 & T_{\max}E_0^{\rm T}M^{\rm T}\\ \star & -T_{\max}R\end{bmatrix} < 0, \tag{48}$$

where

$$\begin{aligned}\Phi_0 &= {\rm He}\{E_1^{\rm T}P(E_2+E_3) - E_2^{\rm T}S_2E_3 + E_0^{\rm T}M^{\rm T}E_2 + (E_1+E_2)^{\rm T}[-L\ AL\ AL+BY]\}\\ &\quad - E_2^{\rm T}S_1E_2 - E_2^{\rm T}\tilde{\Omega}E_2 + \sigma(E_2+E_3)^{\rm T}\tilde{\Omega}(E_2+E_3),\\ \Phi_1 &= 2E_1^{\rm T}S_1E_2 + 2E_1^{\rm T}S_2E_3 + E_3^{\rm T}S_3E_3 + E_1^{\rm T}RE_1,\\ E_1 &= [I\ 0\ 0],\ E_2 = [0\ I\ 0],\ E_3 = [0\ 0\ I],\ E_0 = {\rm col}\{E_2+E_3, E_3\}.\end{aligned}$$

Moreover, the weighted matrix Ω in the ETC (41) is $\Omega = (L^{\rm T})^{-1}\tilde{\Omega}L^{-1}$.

Proof. Taking the derivative of $\mathcal{W}(t)$ yields

$$\begin{aligned}\dot{\mathcal{W}}(t) &= \xi^{\rm T}(t)\Big\{2E_1^{\rm T}P(E_2+E_3) - E_2^{\rm T}S_1E_2 - 2E_2^{\rm T}S_2E_3 - (t-t_k)E_3^{\rm T}S_3E_3\\ &\quad + (t_{k+1}-t)[2E_1^{\rm T}S_1E_2 + 2E_1^{\rm T}S_2E_3 + E_3^{\rm T}S_3E_3 + E_1^{\rm T}RE_1]\Big\}\xi(t) - \int_{t_k}^{t}\dot{\tilde{x}}^{\rm T}(s)R\dot{\tilde{x}}(s){\rm d}s,\end{aligned} \tag{49}$$

where $\xi(t) = {\rm col}\{\dot{\tilde{x}}(t), \tilde{e}(t), \tilde{x}(t_k)\}$. To simplify the presentation, we employ the integral inequality [55, Proposition 3] to bound the integral term above, leading to

$$-\int_{t_k}^{t}\dot{\tilde{x}}^{\rm T}(s)R\dot{\tilde{x}}(s){\rm d}s \leqslant \xi^{\rm T}(t)\big[E_0^{\rm T}M^{\rm T}E_2 + E_2^{\rm T}ME_0 + (t-t_k)E_0^{\rm T}M^{\rm T}R^{-1}ME_0\big]\xi(t), \tag{50}$$

where $M \in \mathbb{R}^{n\times 2n}$. From the closed-loop system (42), one has

$$0 = 2[\dot{\tilde{x}}(t) + \tilde{e}(t)]^{\rm T}[-L\dot{\tilde{x}}(t) + AL\tilde{e}(t) + (A+BK)L\tilde{x}(t_k)]. \tag{51}$$

Combining (49)–(51), together with the ETC (41), and letting $Y = KL$ and $\tilde{\Omega} = L^{\mathrm{T}}\Omega L$, one obtains

$$\dot{\mathcal{W}}(t) \leqslant \xi^{\mathrm{T}}(t)\frac{(t_{k+1}-t)(\Phi_0 + T_k\Phi_1) + (t-t_k)(\Phi_0 + T_k\Phi_2)}{t_{k+1}-t_k}\xi(t), \tag{52}$$

where $\Phi_2 = E_0^{\mathrm{T}} M^{\mathrm{T}} R^{-1} M E_0 - E_3^{\mathrm{T}} S_3 E_3$. Clearly, $\dot{\mathcal{W}}(t) < 0$ if the matrix inequalities in (47) and (48) are satisfied.

Theorems 5 and 6 present two LMI-based algorithms to co-design both the control gain K and the weighted matrix Ω such that the sampled-date system with the ETC (41) is asymptotically stable. Theorem 5 is independent of two parameters $T_{\min}$ and $T_{\max}$, which are the lower and upper bounds of the sampling intervals T_k $(k = 1, 2, \ldots)$, respectively. Although $T_{\min} > 0$ is implicitly ensured by the ETC (41), the upper bound $T_{\max}$ is not involved in Theorem 5. In contrast, Theorem 6 depends on both $T_{\min}$ and $T_{\max}$, making the controller and ETC sensitive to the sampling intervals. This dependence is crucial because $T_{\max}$ plays a significant role in preventing the sampling intervals from becoming excessively large, which is aligned with the principles of the Nyquist-Shannon sampling theorem.

By constructing an alternative looped functional as suggested in [56] and applying the Bessel-Legendre inequality to bound the integral terms, it is possible to derive some co-design criteria that are less conservative than Theorem 6.

It should be pointed out that the co-design method mentioned above can be extended to (dynamic) output feedback scenarios.

3.2 Linear systems with external disturbances

Consider the following system:

$$\begin{cases} \dot{x}(t) = Ax(t) + B_u u(t) + B_w w(t),\ x(t_0) = x_0, \\ z(t) = C_z x(t), \end{cases} \tag{53}$$

where $x(t) \in \mathbb{R}^n, u(t) \in \mathbb{R}^m, z(t) \in \mathbb{R}^{n_z}$, and $w(t) \in \mathbb{R}^{n_w}$ are the system state, control input, controlled output, and the external disturbance, respectively, and A, B_u, B_w, C_y, and C_z are known real matrices. Suppose that (A, B_u) is controllable.

Due to the presence of external disturbances, it is nontrivial to devise an ETC such that Zeno behavior can be excluded. For the co-design issue for the system (53), in the recent years, several results have been proposed [57, 58]. In the sequel, we take a brief review of them.

3.2.1 *Co-design without considering the upper bound of inter-event times*

In [57], the following ETC is proposed:

$$t_{k+1} = \inf\{t > t_k \mid [x^{\mathrm{T}}(t)\ e^{\mathrm{T}}(t)]\Omega\mathrm{col}\{x(t), e(t)\} - \Delta(t) = 0\}, \tag{54a}$$

$$\Delta(t) = \begin{cases} \delta, & t \in [t_k, t_k + \hat{\tau}], \\ \eta e^{-\sigma t}, & \text{otherwise}, \end{cases} \quad \Omega = \begin{bmatrix} -\Omega_1 & \Omega_2 \\ \Omega_2^{\mathrm{T}} & \Omega_3 \end{bmatrix}, \tag{54b}$$

where $t_0 = 0$, $e(t) = x(t) - x(t_k)$, $\eta > 0, \delta > 0, \sigma > 0$, and $\hat{\tau} > 0$ are real parameters, and the real matrices $\Omega_1, \Omega_2, \Omega_3$ satisfy $\Omega_1 > 0$, $\|\Omega_2\| \neq 0$, and $\lambda_{\max}(\Omega_3) \geqslant 0$.

From [35], the ETC (54) with $\Delta(t) \equiv 0$ may exhibit Zeno behavior due to the disturbance $w(t)$ in (53). Thus, the introduction of $\Delta(t)$ aims to avoid the occurrence of Zeno behavior. In fact, it has been proven in [57, Theorem 1] that under the ETC (54), the following closed-loop system of (53) with $u = Kx$:

$$\begin{cases} \dot{x}(t) = (A + B_u K)x(t) + B_u K e(t) + B_w w(t),\ x(t_0) = x_0, \\ z(t) = C_z x(t) \end{cases} \tag{55}$$

has the event-separation property. Moreover, the minimum inter-event time is dependent on the system matrices A, B_u, B_w, control gain K, and event-triggering parameters Ω and δ.

The co-design problem stated in [57] is to jointly design the control gain K and the triggering parameters Ω and $\Delta(t)$ such that the closed-loop system is finite gain $\mathcal{L}_2$-stable and has $\mathcal{L}_2$-gain less than γ for some $\gamma > 0$ in the sense of Definition 1 as follows.

Definition 1. The closed-loop system (55) is finite gain $\mathcal{L}_2$-stable from w to z and has $\mathcal{L}_2$-gain less than γ if there exist two scalars $\gamma > 0$ and $\alpha \geqslant 0$ and a positive semidefinite continuous function β such that

$$\mathcal{J}(\gamma) \triangleq \int_0^{T_0} \|z(s)\|^2 - \gamma^2\|w(s)\|^2 \mathrm{d}s \leqslant \alpha + \beta(x_0),\ \forall T_0 \in [0,\infty),\ \forall w \in \mathcal{L}_2^{n_w},\ \forall x_0 \in \mathbb{R}^n. \tag{56}$$

Theorem 7. For some scalars $\mu_0 > 0, \epsilon_0 > 0, \gamma > 0$, suppose that there exist two real matrices $P > 0$ and K such that

$$\Theta_0 + (\mu_0 + \epsilon_0)I \leqslant 0, \tag{57}$$

$$\Theta_0 \triangleq P(A + B_uK) + (A + B_uK)^{\mathrm{T}}P + \gamma^{-2}PB_wB_w^{\mathrm{T}}P + C_z^{\mathrm{T}}C_z. \tag{58}$$

Choose $\hat{\tau} = \min\{\tau_1, \tau_2\}$, where τ_1 and τ_2 satisfy

$$\aleph(t_k, t_k + \tau_1) = 0.25\|A + B_uK\|^{-2}\|PB_uK\|^{-2}\epsilon_0^2, \tag{59}$$

$$\aleph(t_k, t_k + \tau_2) = 0.5\epsilon_0\|PB_uK\|^{-2}\|B_w\|^{-2}(\gamma_d^2 - \gamma^2), \tag{60}$$

$$\aleph(t_k, t) = 2\int_{t_k}^{t}\int_{t_k}^{s} \mathrm{e}^{2\|B_uK\|(s-\tau)}\mathrm{d}\tau\mathrm{d}s, \tag{61}$$

where $\gamma_d \geqslant \gamma$. Then under the ETC (54) with $\Omega_1 = -\epsilon_0 I$, $\Omega_2 = PB_uK$, and $\Omega_3 = 0$, the closed-loop system is finite gain $\mathcal{L}_2$-stable and has $\mathcal{L}_2$-gain less than $\gamma_d > 0$.

Proof. Let $V(t) = x^{\mathrm{T}}(t)Px(t)$ with $P > 0$. Taking its derivative along with (55) yields

$$\dot{V}(t) \leqslant \begin{bmatrix} x(t) \\ e(t) \end{bmatrix}^{\mathrm{T}} \begin{bmatrix} \Theta_0 & PB_uK \\ \star & 0 \end{bmatrix} \begin{bmatrix} x(t) \\ e(t) \end{bmatrix} + \gamma^2\|w(t)\|^2 - \|z(t)\|^2. \tag{62}$$

Consider two cases: $t \in [t_k, t_k + \hat{\tau}]$ and $t \in [t_k + \hat{\tau}, t_{k+1})$.

Case 1: $t \in [t_k, t_k + \hat{\tau}]$.

Integral both sides of (62) from t_k to t to get

$$\int_{t_k}^{t} \big[\|z(s)\|^2 - \gamma^2\|w(s)\|^2\big]\mathrm{d}s \leqslant \int_{t_k}^{t} \begin{bmatrix} x(s) \\ e(s) \end{bmatrix}^{\mathrm{T}} \begin{bmatrix} \Theta_0 & PB_uK \\ \star & 0 \end{bmatrix} \begin{bmatrix} x(s) \\ e(s) \end{bmatrix} \mathrm{d}s + V(t_k) - V(t). \tag{63}$$

From [57], $e(t)$ satisfies the following inequality:

$$\int_{t_k}^{t} \|e(s)\|^2\mathrm{d}s \leqslant \aleph(t_k, t)\int_{t_k}^{t} (\|A + B_uK\|^2\|x(s)\|^2 + \|B_w\|^2\|w(s)\|^2)\mathrm{d}s, \tag{64}$$

where $\aleph(t_k, t)$ is defined in (61). Note that $\aleph(t_k, t)$ is a monotonically increasing function on t ($\geqslant t_k$). Moreover, direct calculation gives $\aleph(t_k, t) = (2\|B_uK\|)^{-2}[\mathrm{e}^{2\|B_uK\|(t-t_k)} - 2\|B_uK\|(t - t_k) - 1]$. Clearly, $\aleph(t_k, t)$ is a monotonically increasing function on $t - t_k$.

Apply S-procedure to (63) and (64) to obtain, for any scalar $\varepsilon_1 \geqslant 0$,

$$\int_{t_k}^{t} \big[\|z(s)\|^2 - (\gamma^2 + \varepsilon_1\|B_w\|^2\aleph(t_k, t))\|w(s)\|^2\big]\mathrm{d}s \leqslant \int_{t_k}^{t} \begin{bmatrix} x(s) \\ e(s) \end{bmatrix}^{\mathrm{T}} \Theta_1 \begin{bmatrix} x(s) \\ e(s) \end{bmatrix} \mathrm{d}s + V(t_k) - V(t), \tag{65a}$$

$$\Theta_1 \triangleq \begin{bmatrix} \Theta_0 + \varepsilon_1\aleph(t_k, t)\|A + B_uK\|^2 I & PB_uK \\ \star & -\varepsilon_1 I \end{bmatrix}. \tag{65b}$$

Set $\varepsilon_1 = 2\epsilon_0^{-1}\|PB_uK\|^2$. Due to the monotonicity of $\aleph(t_k, t)$ on $t - t_k$, one has

$$\begin{aligned} &\Theta_0 + \varepsilon_1\aleph(t_k, t)\|A + B_uK\|^2 I + \varepsilon_1^{-1}PB_uKK^{\mathrm{T}}B_u^{\mathrm{T}}P \\ &\leqslant \Theta_0 + \varepsilon_1\aleph(t_k, t_k + \tau_1)\|A + B_uK\|^2 I + \varepsilon_1^{-1}PB_uKK^{\mathrm{T}}B_u^{\mathrm{T}}P \\ &\leqslant \Theta_0 + \epsilon_0 I \leqslant -\mu_0 I. \end{aligned} \tag{66}$$

The last inequality above is obtained using (57). Thus, by the Schur complement, $\Theta_1 < 0$ and

$$\begin{bmatrix} x(s) \\ e(s) \end{bmatrix}^{\mathrm{T}} \Theta_1 \begin{bmatrix} x(s) \\ e(s) \end{bmatrix} \mathrm{d}s \leqslant -\mu_0 \|x(s)\|^2. \tag{67}$$

On the other hand, let $\gamma_d \geqslant \gamma$. It follows from (60) that

$$\int_{t_k}^{t} \left[\|z(s)\|^2 - \gamma_d^2 \|w(s)\|^2\right] \mathrm{d}s = \int_{t_k}^{t} \left[\|z(s)\|^2 - (\gamma^2 + \varepsilon_1 \|B_w\|^2 \aleph(t_k, t_k + \tau_2)) \|w(s)\|^2\right] \mathrm{d}s. \tag{68}$$

Therefore, from (65a), (67), and (68), we obtain

$$\int_{t_k}^{t} \left[\|z(s)\|^2 - \gamma_d^2 \|w(s)\|^2\right] \mathrm{d}s \leqslant -\int_{t_k}^{t} \mu_0 \|x(s)\|^2 \mathrm{d}s + V(t_k) - V(t), \ t \in [t_k, t_k + \hat{\tau}]. \tag{69}$$

Case 2: $t \in [t_k + \hat{\tau}, t_{k+1})$.

From (57), we have $\Theta_0 + (\mu_0 + \epsilon_0) I \leqslant 0$. Under the ETC (54) with $\Omega_1 = -\epsilon_0 I$, $\Omega_2 = PB_u K$, and $\Omega_3 = 0$ and for $t \in [t_k + \hat{\tau}, t_{k+1})$, one obtains

$$\begin{bmatrix} x(t) \\ e(t) \end{bmatrix}^{\mathrm{T}} \begin{bmatrix} \Theta_0 & PB_u K \\ \star & 0 \end{bmatrix} \begin{bmatrix} x(t) \\ e(t) \end{bmatrix} \leqslant \begin{bmatrix} x(t) \\ e(t) \end{bmatrix}^{\mathrm{T}} \begin{bmatrix} -\epsilon_0 I & PB_u K \\ \star & 0 \end{bmatrix} \begin{bmatrix} x(t) \\ e(t) \end{bmatrix} - \mu_0 \|x(t)\|^2 \leqslant \eta \mathrm{e}^{-\sigma t} - \mu_0 \|x(t)\|^2. \tag{70}$$

Integrating both sides of (62) from $t_k + \hat{\tau}$ to t yields for $\gamma_d \geqslant \gamma$,

$$\begin{aligned} \int_{t_k+\hat{\tau}}^{t} \left[\|z(s)\|^2 - \gamma_d^2 \|w(s)\|^2\right] \mathrm{d}s &\leqslant \int_{t_k+\hat{\tau}}^{t} \left[\|z(s)\|^2 - \gamma^2 \|w(s)\|^2\right] \mathrm{d}s \\ &\leqslant \int_{t_k+\hat{\tau}}^{t} [\eta \mathrm{e}^{-\sigma s} - \mu_0 \|x(s)\|^2] \mathrm{d}s + V(t_k + \hat{\tau}) - V(t). \end{aligned} \tag{71}$$

From (69) and (71), it is clear that for $\forall t \in [t_k, t_{k+1})$,

$$\begin{aligned} \int_{t_k}^{t} \left[\|z(s)\|^2 - \gamma_d^2 \|w(s)\|^2\right] \mathrm{d}s &= \int_{t_k}^{t+\hat{\tau}} \left[\|z(s)\|^2 - \gamma_d^2 \|w(s)\|^2\right] \mathrm{d}s + \int_{t_k+\hat{\tau}}^{t} \left[\|z(s)\|^2 - \gamma_d^2 \|w(s)\|^2\right] \mathrm{d}s \\ &\leqslant \int_{t_k}^{t} \eta \mathrm{e}^{-\sigma s} \mathrm{d}s - \int_{t_k}^{t} \mu_0 \|x(s)\|^2 \mathrm{d}s + V(t_k) - V(t), \end{aligned} \tag{72}$$

which follows that, for $\forall t > 0$,

$$\int_{0}^{t} \left[\|z(s)\|^2 - \gamma_d^2 \|w(s)\|^2\right] \mathrm{d}s \leqslant V(x_0) + \frac{\eta}{\sigma}. \tag{73}$$

The proof is then completed according to Definition 1.

One of the key innovations of Theorem 7 is the design of the time parameter $\hat{\tau}$ in the ETC (54), which incorporates the monotonically increasing function $\aleph(t_k, t)$ as defined in (61). Notably, the matrix Θ_1 in (65b) is influenced by $\aleph(t_k, t)$. From Definition 1, the function $\aleph(t_k, t)$ is permitted to increase until (i) $\Theta_1 < 0$ and (ii) the desired performance index γ_d is no longer satisfied. This insight is pivotal in the co-design of both the control gain K and the ETC (54).

In the ETC (54), the parameter δ is introduced to ensure the event-separation property, guaranteeing a positive minimum inter-event time. Typically, introducing δ may weaken the stability of the closed-loop system, shifting it from asymptotic stability to practical stability [35]. However, as demonstrated in [57], if there exists a constant $\rho > 0$ such that $\Theta_0 + \rho P + (\mu_0 + \epsilon_0) I \leqslant 0$, the closed-loop system under the ETC (54) with $\sigma > \rho$ remains exponentially stable with a convergence rate $\rho > 0$.

The co-design algorithm presented in Theorem 7 can be viewed as an emulation-based approach. Specifically, one can first design the control gain K such that $\Theta_0 < 0$. Then, using this control gain, the ETC parameters can be determined according to Theorem 7. This aligns with Theorem 7 because, when

$\Theta_0 < 0$, there exists a constant $\varepsilon_0 > 0$ such that $\Theta_0 \leqslant -\varepsilon_0 I$. By setting $\varepsilon_0 = \mu_0 + \epsilon_0$, the condition $\Theta_0 < 0$ leads to the inequality in (10).

In Theorem 7, the scalars γ and γ_d represent the performance indices of the closed-loop system of (53) with $u = Kx$ and the ETC system (55), respectively. The difference between these indices serves as a measure of the performance degradation caused by the ETC (54). On the other hand, from (60), it is possible to design a suitable $\hat{\tau}$ so that the performance index γ_d closely approximates γ.

Besides state feedback control, Ref. [57] also considers observer-based output feedback control. Based on the same line as above, some algorithms are provided to co-design both output feedback control gains and ETC parameters.

3.2.2 *Co-design taking into consideration the upper bound of inter-event times*

Due to external disturbances, the ETC (41) may fail to ensure a positive minimum inter-event time for the system (53). To address this issue, a novel ETC scheme is proposed in [58]. Similar to the analysis above, we set $e(t) = x(t) - x(t_k)$. Then the ETC reads as

$$t_{k+1} = \min\big\{\inf\{t > t_k|\ f(x,e) > 0\}, t_k + T_{\max}\big\}, \tag{74a}$$

$$f(x,e) = \left[\int_{t_k}^{t} e(s)\mathrm{d}s\right]^{\mathrm{T}} \Omega \left[\int_{t_k}^{t} e(s)\mathrm{d}s\right] - \sigma x^{\mathrm{T}}(t_k)\Omega x(t_k), \tag{74b}$$

where $\Omega > 0$ is a weighted matrix and $\sigma > 0$ is a threshold. The parameter $T_{\max} > 0$ is introduced to ensure a finite maximum inter-event time, i.e., $t_{k+1} - t_k \leqslant T_{\max}$, $\forall k \in \mathbb{Z}_{\geqslant 0}$, which aligns with the principles of the Nyquist-Shannon sampling theorem.

If setting $\Omega = I$, the physical meaning of the ETC (74a) is that an event is triggered once $\| \int_{t_k}^{t} e(s)\mathrm{d}s\|^2$ is greater than $\sigma\|x(t_k)\|^2$ (or once the accumulation of the error is greater than the σ times of the last sampled state).

As proven in [58], the ETC (74a) can provide an explicit expression on the minimum inter-event time. To make it clear, perform a Taylor expansion of $e(t)$ at t_k to get

$$e(t) = x(t) - x(t_k) = \dot{x}(t_k)(t - t_k) + o(t - t_k), \tag{75}$$

where $o(t-t_k)$ satisfies $\lim_{t\to t_k^+} \frac{o(t-t_k)}{t-t_k} = 0$, which implies that there exists $\beta_0 > 0$ such that

$$\|\Omega^{\frac{1}{2}} o(t-t_k)\| \leqslant \beta_0 \|\Omega^{\frac{1}{2}} x(t_k)\|(t-t_k),\ t \in [t_k, t_{k+1}]. \tag{76}$$

Then it follows from (74a), (75), and (76) that

$$\begin{aligned}
\sqrt{\sigma}\|\Omega^{\frac{1}{2}} x(t_k)\| &< \left\|\Omega^{\frac{1}{2}} \int_{t_k}^{t_{k+1}} e(s)\mathrm{d}s\right\| \\
&= \left\|\Omega^{\frac{1}{2}} \int_{t_k}^{t_{k+1}} [\dot{x}(t_k)(s-t_k) + o(s-t_k)]\mathrm{d}s\right\| \\
&\leqslant \left\|\Omega^{\frac{1}{2}} \int_{t_k}^{t_{k+1}} \dot{x}(t_k)(s-t_k)\mathrm{d}s\right\| + \int_{t_k}^{t_{k+1}} \|\Omega^{\frac{1}{2}} o(s-t_k)\|\mathrm{d}s \\
&\leqslant 0.5\big(\|\Omega^{\frac{1}{2}}\dot{x}(t_k)\| + \beta_0\|\Omega^{\frac{1}{2}} x(t_k)\|\big)(t_{k+1}-t_k)^2
\end{aligned} \tag{77}$$

which leads to

$$(t_{k+1} - t_k)^2 > \frac{2\sqrt{\sigma}\|\Omega^{\frac{1}{2}} x(t_k)\|}{\|\Omega^{\frac{1}{2}}\dot{x}(t_k)\| + \beta_0\|\Omega^{\frac{1}{2}} x(t_k)\|}.$$

Note that $\dot{x}(t_k) = (A + B_u K)x(t_k) + B_w w(t_k)$. If $w \in \mathcal{L}_2^{n_w}$ or $\|w(t)\| \leqslant \beta_1$ for $\beta_1 > 0$, then $\|\Omega^{\frac{1}{2}}\dot{x}(t_k)\| \leqslant \|\Omega^{\frac{1}{2}}(A + B_u K)x(t_k)\| + \beta_1\|B_w\|$, which immediately yields

$$t_{k+1} - t_k > \sqrt{\frac{2\sqrt{\sigma}\|\Omega^{\frac{1}{2}} x(t_k)\|}{\|\Omega^{\frac{1}{2}}(A + B_u K)x(t_k)\| + \beta_1\|B_w\| + \beta_0\|\Omega^{\frac{1}{2}} x(t_k)\|}}. \tag{78}$$

From (78), it is clear that an explicit lower bound of the inter-event time $T_k = t_{k+1} - t_k$ is obtained, which is positive only if $x(t_k) \neq 0$.

The co-design problem addressed in [58] is to design a control gain K and a weighted matrix $\Omega > 0$ for a certain threshold $\sigma > 0$ such that

(i) the closed-loop system (55) with $w(t) \equiv 0$ is asymptotically stable, and

(ii) when $w(t) \neq 0$, under the zero initial condition $x_0 = 0$, the inequality $\mathscr{J}(\gamma) < 0$ holds for a prescribed $\gamma > 0$, where $\mathscr{J}(\gamma)$ is defined in (56).

If both (i) and (ii) are satisfied, it is common to call that the closed-loop system (55) achieves an H_∞ performance level γ.

By constructing an ETC-dependent looped functional, a solution to the problem above is obtained, which is stated in the following. More details are referred to [58].

Theorem 8 ([58]). For given constants $\gamma > 0, \sigma > 0$, and real scalars ϵ_i $(i = 1, 2)$, the closed-loop system (55) achieves an H_∞ performance level γ if there exist real matrices $\tilde{\Omega} > 0, P > 0, R_1 > 0, R_2 > 0$, real symmetric matrices Q_2, Q_3, and real matrices $Q_1, \mathcal{M}_1, \mathcal{M}_2, N_1, N_2, X$, and Y with appropriate dimensions such that, for $T_k \in \{T_{\min}, T_{\max}\}$,

$$\begin{bmatrix} \daleth_{11} & \star & \star & \star \\ B_w^{\mathrm{T}}\Im_0 & -\gamma^2 I & \star & \star \\ C_z X & 0 & -I & \star \\ T_k\mathcal{M}_2 & 0 & 0 & -T_k\mathcal{R}_2 \end{bmatrix} < 0, \quad \begin{bmatrix} \daleth_{21} & \star & \star & \star \\ B_w^{\mathrm{T}}\Im_0 & -\gamma^2 I & \star & \star \\ C_z X e_2 & 0 & -I & \star \\ T_k\mathcal{M}_1 & 0 & 0 & -T_k\mathcal{R}_1 \end{bmatrix} < 0, \tag{79}$$

where $\Im_0 = e_1 + \epsilon_1 e_2 + \epsilon_2 e_3$, $\mathcal{R}_i = \mathrm{diag}\{R_i, 3R_i\}$, and

$$\begin{aligned} &\daleth_{11} = \Phi_1 + \Phi_2 + T_k[\Gamma_1 - \mathrm{He}\{N_2^{\mathrm{T}} e_8\}], \ \daleth_{21} = \Phi_1 + \Phi_2 + T_k[\Gamma_2 + \mathrm{He}\{N_1^{\mathrm{T}}(e_3 - e_7)\}], \\ &\Phi_1 = \mathrm{He}\{e_2^{\mathrm{T}} P e_1 + C_1^{\mathrm{T}} Q_1 C_{20} + C_{51}^{\mathrm{T}} Q_2 C_{61} - C_{52}^{\mathrm{T}} Q_2 C_{62} + \mathcal{M}_1^{\mathrm{T}}\Theta\mathscr{C}_1 + \mathcal{M}_2^{\mathrm{T}}\Theta\mathscr{C}_2\}, \\ &\Phi_2 = \sigma e_3^{\mathrm{T}}\Omega e_3 - e_5^{\mathrm{T}}\Omega e_5 + \mathrm{He}\{N_1^{\mathrm{T}} e_5 + N_2^{\mathrm{T}} e_6 + \Im_0^{\mathrm{T}}(-Xe_1 + AXe_2 + B_u Y e_3)\}, \\ &\Gamma_1 = \mathrm{He}\{C_1^{\mathrm{T}} Q_1 C_{22} + C_3^{\mathrm{T}} Q_1 C_{42}\} + C_7^{\mathrm{T}} Q_3 C_7 + e_1^{\mathrm{T}} R_1 e_1, \\ &\Gamma_2 = \mathrm{He}\{C_1^{\mathrm{T}} Q_1 C_{21} + C_3^{\mathrm{T}} Q_1 C_{41}\} + e_1^{\mathrm{T}} R_2 e_1 - C_7^{\mathrm{T}} Q_3 C_7 \end{aligned}$$

with $\Theta := \left[\begin{smallmatrix} I & -I & 0 \\ I & I & -2I \end{smallmatrix}\right]$, $\mathscr{C}_1 = \mathrm{col}\{e_2, e_3, e_7\}$, $\mathscr{C}_2 = \mathrm{col}\{e_4, e_2, e_8\}$, $C_1 = \mathrm{col}\{e_2, e_3, e_4, e_5, e_6\}$, and

$$\begin{aligned} &C_{20} = \mathrm{col}\{e_3 - e_2, -e_5, e_4 - e_2, e_6\}, C_{21} = \mathrm{col}\{0, 0, -e_1, -e_2\}, \\ &C_{22} = \mathrm{col}\{e_1, e_2 - e_3, 0, 0\}, C_3 = \mathrm{col}\{e_1, 0, 0, e_2 - e_3, -e_2\}, \\ &C_{41} = \mathrm{col}\{0, 0, e_4 - e_2, e_6\}, \ C_{42} = \mathrm{col}\{e_2 - e_3, e_5, 0, 0\}, \\ &C_{51} = \mathrm{col}\{e_1, e_2 - e_3\}, \quad C_{52} = \mathrm{col}\{e_2 - e_3, e_5\}, \\ &C_{61} = \mathrm{col}\{e_4 - e_2, e_6\}, C_{62} = \mathrm{col}\{e_1, e_2\}, C_7 = \mathrm{col}\{e_3, e_4\}, \\ &\ e_1 = [I\ 0\ 0\ 0\ 0\ 0\ 0\ 0], \ e_2 = [0\ I\ 0\ 0\ 0\ 0\ 0\ 0], \ldots, e_8 = [0\ 0\ 0\ 0\ 0\ 0\ 0\ I]. \end{aligned}$$

Moreover, the control gain and the weighted matrix Ω in the ETC (74a) are calculated from $K = YX^{-1}$ and $\Omega = (X^{-1})^{\mathrm{T}}\tilde{\Omega}X^{-1}$.

Theorems 7 and 8 present two methods to the co-design issue for the system (53) in the presence of external disturbances. Theorem 7 emphasizes on the design of the ETC parameter $\hat{\tau} > 0$ such that Zeno behavior is free. This theorem generally follows an emulation-based approach, which may sometimes shift the stability of the closed-loop system to practical stability. On the other hand, Theorem 8 introduces an LMI-based algorithm to co-design both control gains and ETC parameters. Under the designed controller, the closed-loop system is asymptotically stable. Moreover, the designed ETC also ensures the exclusion of Zeno behavior for the disturbed system (53).

3.3 Co-design of dynamic output feedback controllers and ETC schemes

Event-triggered dynamic output feedback (DOF) control, incorporating an event-triggered transmission scheme, is explored in [59, 60], allowing for the joint design of DOF control gains and ETC parameters. However, several limitations persist. First, the system measurements are sampled uniformly rather than

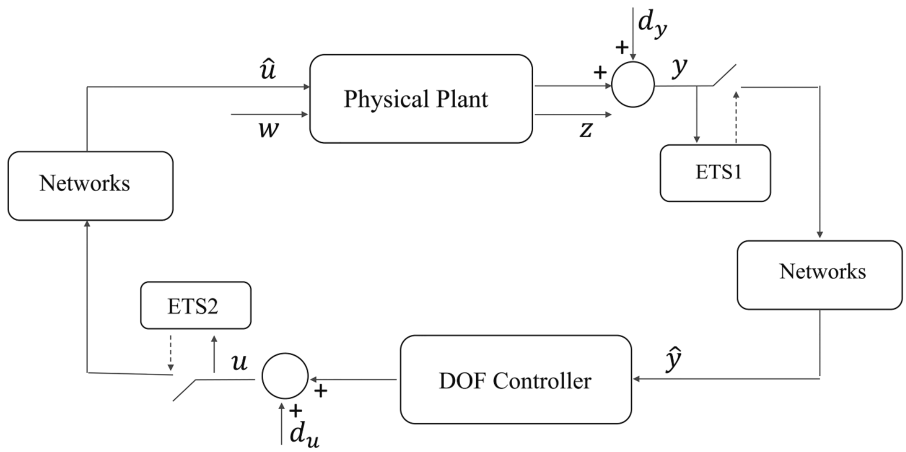

Figure 1 Diagram of event-triggered dynamic output feedback control.

event-triggered. Second, control signals are transmitted to the physical plant by point-to-point wiring instead of through communication networks. Consequently, no sampling is needed for the output of the DOF controller. To address these limitations, significant effort has been made, e.g., [61–64]. Specifically, a hybrid system model is proposed to tackle the co-design challenge under an event-triggered sampling scheme.

Consider the DOF control of networked systems shown in Figure 1, where the physical plant and the DOF controller are described, respectively, by

$$\text{Physical plant:}\ \begin{cases}\dot{\bar{x}}(t) = A\bar{x}(t) + B_u u(t_j^u) + B_w w(t),\ \bar{x}(t_0) = \bar{x}_0,\\ y(t) = C\bar{x}(t) + d_y(t),\end{cases} \qquad t \in [t_j^u, t_{j+1}^u), \tag{80}$$

$$\text{Controller:}\ \begin{cases}\dot{x}_c(t) = A_c x_c(t) + B_c y(t_i^y),\\ u(t) = C_c x_c + d_u(t),\end{cases} \qquad t \in [t_i^y, t_{i+1}^y), \tag{81}$$

where $\bar{x}, u, w$ are the state, control input, and external disturbances of the physical plant, and y, d_y are the system measurement output and additional noise; x_c is the state of the controller and d_u is the noise imposed on u. In Figure 1, two event-triggered schemes, namely ETS1 and ETS2, are inserted into the S-C (sensor to controller) and the C-A (controller to actuator) communication channels, respectively, to sample system measurements and control inputs before transmitted through communication channels. With ETS1 and ETS2, the sampling instants $\{t_i^y | i = 1, 2, \ldots\}$ and $\{t_j^u | j = 1, 2, \ldots\}$ are determined by

$$\text{ETS1:}\ t_{i+1}^y = \inf\left\{t \geqslant t_i^y + T_y \middle| \|e_y(t)\| \geqslant \rho_y \|y(t)\|\right\},\quad e_y(t) = y(t_i^y) - y(t),\quad t_0^y = t_0, \tag{82}$$

$$\text{ETS2:}\ t_{j+1}^u = \inf\left\{t \geqslant t_j^u + T_u \middle| \|e_u(t)\| \geqslant \rho_u \|u(t)\|\right\},\quad e_u(t) = u(t_j^u) - u(t),\quad t_0^u = 0, \tag{83}$$

where T_y and T_u are two positive real numbers serving as the minimum inter-event times, i.e., $T_v = \min\{t_{i+1}^v - t_i^v \big| i = 0, 1, 2, \ldots\}$ with $v \in \{y, u\}$. It should be mentioned that ETS1 and ETS2 work not necessarily synchronically, which means that t_i^y may not be equal to t_i^u.

Introduce two timers $\tau_y(t) = t - t_i^y,\ t \in [t_i^y, t_{i+1}^y]$ and $\tau_u(t) = t - t_j^u,\ t \in [t_j^u, t_{j+1}^u]$ to calculate the time elapses from the last sampling instants of ETS1 and ETS2, respectively. Then the resultant closed-loop system can be described by

$$\begin{cases} \dot{\bar{x}}(t) = A\bar{x}(t) + B_u[e_u(t) + C_c x_c + d_u(t)] + B_w w(t), & t \in [t_j^u, t_{j+1}^u], \\ \dot{x}_c(t) = A_c x_c(t) + B_c[e_y(t) + C\bar{x}(t) + d_y(t)], & t \in [t_i^y, t_{i+1}^y], \\ \dot{e}_y(t) = -C\big[A\bar{x}(t) + B_u(e_u(t) + C_c x_c + d_u(t)) + B_w w(t)\big] - \dot{d}_y(t), & t \in [t_i^y, t_{i+1}^y], \\ \dot{e}_u(t) = -C_c\big[A_c x_c(t) + B_c(e_y(t) + C\bar{x}(t) + d_y(t))\big] - \dot{d}_u(t), & t \in [t_j^u, t_{j+1}^u], \\ e_y((t_i^y)^+) = 0,\ e_u((t_j^u)^+) = 0, & \\ \dot{\tau}_y(t) = 1, & t \in [t_i^y, t_{i+1}^y], \\ \dot{\tau}_u(t) = 1, & t \in [t_j^u, t_{j+1}^u], \\ \tau_y((t_i^y)^+) = 0,\ \tau_u((t_j^u)^+) = 0. & \end{cases} \tag{84}$$

Due to the asynchronism of ETS1 and ETS2, it is not an easy task to get an exact time sequence from the sampling sampling instants $\{t_i^y, t_j^u | i, j = 1, 2, \ldots\}$ for stability analysis of the ETC system (84). To cope with this difficulty, a hybrid system model is presented in [62]. In doing so, define the flow and jump sets as

$$\mathcal{S}_{y1} := \big\{\chi(t) |\ \|e_y(t)\| \leqslant \rho_y \|y(t)\| \ \text{ or } \ \tau_y(t) \in [0, T_y]\big\}, \tag{85a}$$

$$\mathcal{S}_{y2} := \big\{\chi(t) |\ \|e_y(t)\| \geqslant \rho_y \|y(t)\| \ \text{ and } \ \tau_y(t) \geqslant T_y\big\}, \tag{85b}$$

$$\mathcal{S}_{u1} := \big\{\chi(t) |\ \|e_u(t)\| \leqslant \rho_u \|u(t)\| \ \text{ or } \ \tau_u(t) \in [0, T_u]\big\}, \tag{85c}$$

$$\mathcal{S}_{u2} := \big\{\chi(t) |\ \|e_u(t)\| \geqslant \rho_u \|u(t)\| \ \text{ and } \ \tau_u(t) \geqslant T_u\big\}, \tag{85d}$$

where $\chi(t) = \mathrm{col}\{x(t), e_y(t), e_u(t), \tau_y(t), \tau_u(t)\}$ with $x(t) = \mathrm{col}\{\bar{x}(t), x_c(t)\}$.

Then the closed-loop system (84) can be reformulated as

$$\dot{\chi}(t) = \begin{bmatrix} \mathcal{A}x(t) + \mathcal{B}_y e_y(t) + \mathcal{B}_u e_u(t) + \mathcal{B}_{\bar{w}_1}\bar{w}_1(t) \\ -C_y\mathcal{A}x(t) - C_y\mathcal{B}_u e_u(t) - C_y\mathcal{B}_{\bar{w}_1}\bar{w}_1(t) + \mathcal{I}_1\bar{w}_2(t) \\ -C_u\mathcal{A}x(t) - C_u\mathcal{B}_y e_y(t) - C_u\mathcal{B}_{\bar{w}_1}\bar{w}_1(t) + \mathcal{I}_2\bar{w}_2(t) \\ 1 \\ 1 \end{bmatrix}, \qquad \chi(t) \in \mathcal{S}_{y1} \cap \mathcal{S}_{u1}, \tag{86a}$$

$$\chi(t^+) \in \begin{cases} \big\{\mathrm{col}\{\chi(t), 0, e_u, 0, \tau_u\}\big\}, & \chi(t) \in \mathcal{S}_{y2} \backslash \mathcal{S}_{u2}, \\ \big\{\mathrm{col}\{\chi(t), e_y, 0, \tau_y, 0\}\big\}, & \chi(t) \in \mathcal{S}_{u2} \backslash \mathcal{S}_{y2}, \\ \big\{\mathrm{col}\{\chi(t), 0, e_u, 0, \tau_u\},\ \mathrm{col}\{\chi(t), 0, e_u, 0, \tau_u\}\big\}, & \chi(t) \in \mathcal{S}_{y2} \cup \mathcal{S}_{u2}, \end{cases} \tag{86b}$$

where $C_y = [C\ 0]$, $C_u = [0\ C_c]$, $\bar{w}_1(t) = \mathrm{col}\{w(t), d_y(t), d_u(t)\}$, $\bar{w}_2(t) = \mathrm{col}\{\dot{d}_y(t), \dot{d}_u(t)\}$,

$$\mathcal{A} = \begin{bmatrix} A & B_u C_c \\ B_c C & A_c \end{bmatrix},\ \mathcal{B}_y = \begin{bmatrix} 0 \\ B_c \end{bmatrix},\ \mathcal{B}_u = \begin{bmatrix} B_u \\ 0 \end{bmatrix},\ \mathcal{B}_{\bar{w}_1} = \begin{bmatrix} B_w & 0 & B_u \\ 0 & B_c & 0 \end{bmatrix},\ \mathcal{I}_1 = [-I\ 0],\ \mathcal{I}_2 = [0\ \ -I].$$

The system (86) represents a hybrid model of the closed-loop system that connects (80) with (81) under two event-triggered schemes, ETS1 and ETS2. When no events are triggered by either ETS1 or ETS2, which means that $\chi(t) \in \mathcal{S}_{y1} \cap \mathcal{S}_{u1}$, the solution $\chi(t)$ to the system (86) flows smoothly according to (86a). However, when either ETS1 or ETS2 triggers an event, i.e., $\chi(t) \in \mathcal{S}_{y2} \backslash \mathcal{S}_{u2}$ or $\chi(t) \in \mathcal{S}_{u2} \backslash \mathcal{S}_{y2}$, $\chi(t)$ experiences a jump. When both ETS1 and ETS2 trigger events simultaneously, i.e., $\chi(t) \in \mathcal{S}_{y2} \cup \mathcal{S}_{u2}$, the solution $\chi(t)$ undergoes two successive jumps as described in (86b).

Using a Lyapunov-like method, a sufficient condition is derived to ensure that the closed-loop system (86) is $\mathcal{L}_2$ stable with a specified $\mathcal{L}_2$ gain. For more details, refer to [62, Proposition 1] and [63, Proposition 1]. Moreover, based on the obtained sufficient condition, an LMI-based algorithm is developed to jointly design both the DOF controller gains A_c, B_c, and C_c, and the event-triggered parameters ρ_y, ρ_u, T_y, and T_u, as detailed in [63, Theorem 3]. An improved version of this algorithm is provided in [64, Theorem 6].

The hybrid system method paves an effective way to deal with the co-design issue arising from event-triggered DOF control. It enables two event-triggered schemes, ETS1 and ETS2, to operate asynchronously, which is commonly regarded as a hard nut to crack. However, both ETS1 and ETS2 adopt a similar approach to time-regulated ETC by deliberately introducing positive constants, T_y and T_u, to exclude Zeno behavior. Devising a natural event-triggered scheme for the event-triggered DOF control remains a significant challenge. On the other hand, in the hybrid system method above, a strong constraint is imposed on the noises $d_y(t)$ and $d_u(t)$ that are absolutely continuous and differentiable, which may not hold in practical scenarios.

4 Event-triggered observer-based output feedback control

When system states are not available, a state observer is usually used to reconstruct system states based on system measurements. The traditional observer-based control system is described by

$$\text{System:} \quad \begin{cases} \dot{x}_s(t) = Ax_s(t) + Bu(t),\ x_s(t_0) = x_{s0}, \\ y(t) = Cx_s(t), \end{cases} \tag{87}$$

$$\text{Observer:} \quad \dot{x}_o(t) = Ax_o(t) + Bu(t) + L(Cx_o(t) - y(t)), \tag{88}$$

$$\text{Controller:} \quad u(t) = Kx_o(t), \tag{89}$$

where $x_s(t)$, $u(t)$, and $y(t)$, respectively, are the system state, control input, and system measurement, and $x_o(t)$ is the observer state. It is assumed that the matrix pair (A, B) is controllable and (A, C) is observable.

The classical observer-based control problem follows a separation principle. Specifically, one can independently determine matrices L and K such that both $A + LC$ and $A + BK$ are Hurwitz. Then the resulting L and K can ensure that the closed-loop system associated with (87)–(89) is asymptotically stable [65]. This point can be clearly implied from the following error system with $e(t) = x_o(t) - x_s(t)$:

$$\begin{bmatrix} \dot{x}_s(t) \\ \dot{e}(t) \end{bmatrix} = \begin{bmatrix} A + BK & BK \\ 0 & A + LC \end{bmatrix} \begin{bmatrix} x_s(t) \\ e(t) \end{bmatrix}. \tag{90}$$

However, in networked environments, system measurements and control signals are typically sampled through event-triggered schemes and then transmitted over communication channels. This necessitates a reevaluation of classical observer-based output feedback control methods before they can be effectively applied to networked systems. Over the past decade, inspired by the pioneering work of [18], there has been growing interest in event-triggered output feedback control, leading to the development of numerous significant results, as seen in [66–70]. Notably, it is shown in [65] that some form of separation principle still holds for event-triggered observer-based output feedback control, which is briefly reviewed in the following subsections.

4.1 Separation principle regardless of Zeno behavior

The framework of event-triggered observer-based output feedback control is shown in Figure 2, where the physical plant and the observer are described in (87) and (88), respectively. ETS1 and ETS2 are two event-triggered schemes placed in the S-O (sensor-observer) channel and the O-A (observer-actuator) channel, respectively, which are given as

$$\text{ETS1:} \quad t^y_{i+1} = \inf\{t > t^y_i \mid \mathcal{G}_1(y(t)) \geqslant 0\}, \quad t^y_0 = t_0, \tag{91}$$

$$\text{ETS2:} \quad t^o_{j+1} = \inf\{t > t^o_j \mid \mathcal{G}_2(x_o(t)) \geqslant 0\}, \quad t^o_0 = t_0, \tag{92}$$

where $\mathcal{G}_1(\cdot)$ and $\mathcal{G}_2(\cdot)$ are two predefined event-triggering functions. Let the recent sampling instants be t^y_i and t^o_j. Define $s_l = \max\{t^y_i, t^o_j\}$ and $s_{l+1} = \min\{t^y_{i+1}, t^o_{j+1}\}$. Then for $t \in [s_l, s_{l+1})$,

$$\begin{bmatrix} \dot{x}_s(t) \\ \dot{e}(t) \end{bmatrix} = \begin{bmatrix} A + BK & BK \\ 0 & A + LC \end{bmatrix} \begin{bmatrix} x_s(t) \\ e(t) \end{bmatrix} + \begin{bmatrix} BKe_o(t) \\ -Le_y(t) \end{bmatrix}, \tag{93}$$

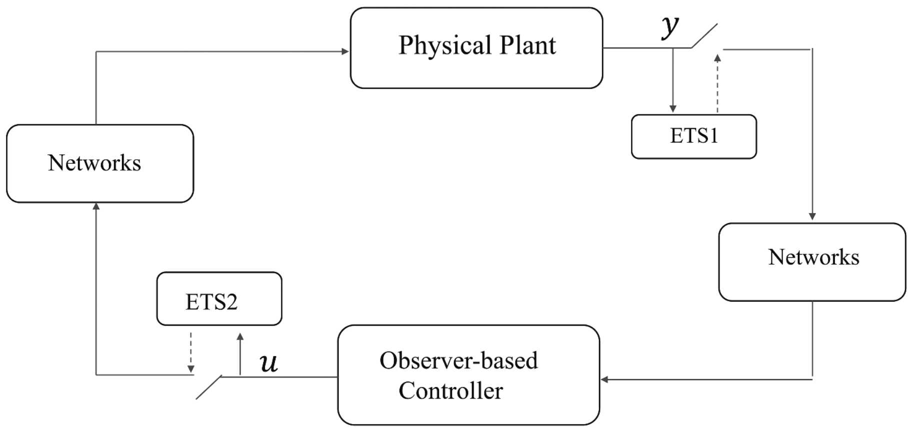

Figure 2 Diagram of event-triggered observer-based output feedback control.

where $e_o(t) = x_o(t_j^o) - x_o(t)$ and $e_y(t) = y(t_i^y) - y(t)$. Clearly, if there are neither event-triggered schemes nor communication channels, both the error dynamics $e_o(t)$ and $e_y(t)$ are always zero. In this situation, Eq. (93) reduces exactly to the one in (90), which means that the separation principle works.

As one of contributions in [65], it is proven that the separation principle still holds even though both the error dynamics $e_o(t)$ and $e_y(t)$ are not zero. In other words, one can separately design $(L, \mathcal{G}_1(\cdot))$ and $(K, \mathcal{G}_2(\cdot))$ such that the system (93) is asymptotically stable, which can be seen from the following result.

Theorem 9 ([65])**.** The event-triggered system (93) is asymptotically stable if there exist scalars $\sigma_v > 0$ and real matrices $P_v > 0, D_v > 0, Q_v > 0$ with $v \in \{y, o\}$, and real matrices K and L such that

$$D_y + P_y(A + LC) + (A + LC)^{\mathrm{T}} P_y + \sigma_y^{-1} C^{\mathrm{T}} C + Q_y < 0, \tag{94a}$$

$$D_o + P_o(A + BK) + (A + BK)^{\mathrm{T}} P_o + \sigma_o I + Q_o < 0. \tag{94b}$$

Moreover, the event-triggering functions $\mathcal{G}_1(\cdot)$ and $\mathcal{G}_2(\cdot)$ can be designed as

$$\mathcal{G}_1(y(t)) = \|D_y^{-\frac{1}{2}} P_y L[e_y(t) + Ce_o(t)]\| - \sqrt{\lambda_y/\sigma_y}\|Ce(t)\|, \tag{95a}$$

$$\mathcal{G}_2(x_o(t)) = \|D_o^{-\frac{1}{2}} P_o BK e_o(t)\| - \sqrt{\lambda_o \sigma_o}\|x_o(t)\|, \tag{95b}$$

where $\lambda_v \in [0, 1)$ for $v \in \{y, o\}$.

From Theorem 9, one can jointly design both the observer gain L and the event-triggering function $\mathcal{G}_1(y(t))$ using (94a) and (95a), as well as co-design the control gain K and the event-triggering function $\mathcal{G}_2(x_o(t))$ based on (94b) and (95b). Clearly, the design procedure outlined above follows the separation principle.

It is important to note that the event-triggered schemes designed in Theorem 9 may result in Zeno behavior, even in the absence of external disturbances. This issue arises because the output matrix C is usually not invertible, meaning that $Cx = 0$ is possible even when $x \neq 0$. In order to exclude Zeno behavior, both ETS1 and ETS2 are modified in [65] by adopting the approach introduced in [57].

4.2 Modified ETS1 and ETS2 for Zeno behavior exclusion

Similar to [57], two scalars, δ_y and δ_o are introduced to modify (95) as

$$\widehat{\mathcal{G}}_1(y(t)) = \begin{cases} \|D_y^{-\frac{1}{2}} P_y L e_y(t)\| - c_y\sqrt{\lambda_y/\sigma_y}\delta_y, & t_i^y \leqslant t < t_i^y + \hat{\tau}_y, \\ \|D_y^{-\frac{1}{2}} P_y L e_y(t)\| - c_y\sqrt{\lambda_y/\sigma_y}\|y(t)\|, & t_i^y + \hat{\tau}_y \leqslant t < t_{i+1}^y, \end{cases} \tag{96a}$$

$$\widehat{\mathcal{G}}_2(x_o(t)) = \begin{cases} \|D_o^{-\frac{1}{2}} P_o BK e_o(t)\| - c_o\sqrt{\lambda_o\sigma_o}\delta_o, & t_j^o \leqslant t < t_j^o + \hat{\tau}_o, \\ \|D_o^{-\frac{1}{2}} P_o BK e_o(t)\| - c_o\sqrt{\lambda_o\sigma_o}\|x_o(t)\|, & t_j^o + \hat{\tau}_o \leqslant t < t_{j+1}^o, \end{cases} \tag{96b}$$

where $c_y, c_o \in (0,1)$, $\hat{\tau}_y > 0$, and $\hat{\tau}_o > 0$. The introduction of δ_y and δ_o can ensure Zeno freeness. In fact, if $\|x_s(t)\|$ is bounded, there exists a constant $\ell_0 > 0$ such that $\frac{\mathrm{d}}{\mathrm{d}t}\|D_y^{-\frac{1}{2}}P_yLe_y(t)\| \leqslant \ell_0$. Then

$$\int_{t_i^y}^{t_i^y+\hat{\tau}_y} \frac{\mathrm{d}}{\mathrm{d}t}\|D_y^{-\frac{1}{2}}P_yLe_y(t)\|\mathrm{d}t = c_y\sqrt{\lambda_y/\sigma_y}\delta_y \leqslant \ell_0\hat{\tau}_y \Longrightarrow \hat{\tau}_y \geqslant (c_y/\ell_0)\sqrt{\lambda_y/\sigma_y}\delta_y > 0. \tag{97}$$

Similarly, $\hat{\tau}_o > 0$ can also be ensured by ETS2 with (96b).

With the modified ETS1 and ETS2 in (96), the objective is to design two parameters, $\hat{\tau}_y$ and $\hat{\tau}_o$, such that the closed-loop system (93) is exponentially stable. In doing so, a novel approach is presented in [65].

Step 1: Choose the Lyapunov function as $V(t) = x_s^{\mathrm{T}}(t)P_ox_s(t) + \theta e^{\mathrm{T}}(t)P_ye(t)$, where $\theta > 0$, and P_y and P_o satisfy (94a) and (94b), respectively. Taking its derivative along with (93) yields

$$\begin{aligned}\dot{V}(t)|_{(93)} &\leqslant \mathcal{F}(e_y(t), e_o(t)) + \zeta^{\mathrm{T}}(t)\begin{bmatrix}\mathrm{He}\{P_o(A+BK)\} + D_o & P_oBK \\ \star & \mathrm{He}\{\theta P_y(A+LC)\} + \theta D_y\end{bmatrix}\zeta(t) \\ &\leqslant \mathcal{F}(e_y(t), e_o(t)) + \zeta^{\mathrm{T}}(t)\begin{bmatrix}-Q_o - \sigma_oI & P_oBK \\ \star & -\theta(\sigma_y^{-1}C^{\mathrm{T}}C + Q_y)\end{bmatrix}\zeta(t),\end{aligned} \tag{98}$$

where $\zeta(t) = \mathrm{col}\{x_s(t), e(t)\}$ and

$$\mathcal{F}(e_y(t), e_o(t)) = \theta\|D_y^{-\frac{1}{2}}P_yLe_y(t)\|^2 + \|D_o^{-\frac{1}{2}}P_oBKe_o(t)\|^2.$$

Let $\mu \in (0,1)$ be a constant. Let $\lambda^* = (1-\mu)\min\{\frac{\lambda_{\min}(Q_y)}{\lambda_{\max}(P_y)}, \frac{\lambda_{\min}(Q_o)}{\lambda_{\max}(P_o)}\}$. Then $(1-\mu)Q_y \geqslant \lambda^*P_y$ and $(1-\mu)Q_o \geqslant \lambda^*P_o$, which lead to $-(1-\mu)x_s^{\mathrm{T}}(t)Q_ox_s(t) - (1-\mu)\theta e^{\mathrm{T}}(t)Q_ye(t) \leqslant -\lambda^*V(t)$. Thus, it follows from (98) that

$$\begin{aligned}\frac{\mathrm{d}}{\mathrm{d}t}V(t)|_{(93)} &\leqslant -\lambda^*V(t) + \mathcal{F}(e_y(t), e_o(t)) + \zeta^{\mathrm{T}}(t)\begin{bmatrix}-\mu Q_o - \sigma_oI & P_oBK \\ \star & -\theta(\sigma_y^{-1}C^{\mathrm{T}}C + \mu Q_y)\end{bmatrix}\zeta(t) \\ &\leqslant -\lambda^*V(t) + \zeta^{\mathrm{T}}(t)\mathcal{M}\zeta(t) + \mathcal{F}(e_y(t), e_o(t)) - \zeta^{\mathrm{T}}(t)\mathcal{N}\zeta(t),\end{aligned} \tag{99}$$

where

$$\mathcal{M} = \begin{bmatrix}-\mu Q_o + \frac{\theta\lambda_y}{\sigma_y}C^{\mathrm{T}}C & P_oBK + \lambda_o\sigma_oI \\ \star & -\theta(\sigma_y^{-1}C^{\mathrm{T}}C + \mu Q_y) + \lambda_o\sigma_oI\end{bmatrix}, \quad \mathcal{N} = \begin{bmatrix}\frac{\theta\lambda_y}{\sigma_y}C^{\mathrm{T}}C + \lambda_o\sigma_oI & \lambda_o\sigma_oI \\ \star & \lambda_o\sigma_oI\end{bmatrix}. \tag{100}$$

Integrate both sides of (99) from 0 to t to get

$$V(t) \leqslant V(0)\mathrm{e}^{-\lambda^*t} + \mathrm{e}^{-\lambda^*t}\int_0^t \zeta^{\mathrm{T}}(s)\mathcal{M}\zeta(s)\mathrm{d}s + \mathrm{e}^{-\lambda^*t}\int_0^t [\mathcal{F}(e_y(s), e_o(s)) - \zeta^{\mathrm{T}}(s)\mathcal{N}\zeta(s)]\mathrm{d}s. \tag{101}$$

If $\mathcal{M} < 0$ and $\int_0^t[\mathcal{F}(e_y(s), e_o(s)) - \zeta^{\mathrm{T}}(s)\mathcal{N}\zeta(s)]\mathrm{d}s \leqslant 0$, then from (101) it is clear that $\|e(t)\|^2 \leqslant V(0)\mathrm{e}^{-\lambda^*t}$, meaning that the system (93) is exponentially stable with a decay rate of $\lambda^* > 0$.

Step 2: Design two parameters, $\hat{\tau}_y$ and $\hat{\tau}_o$, such that $\int_0^t[\mathcal{F}(e_y(s), e_o(s)) - \zeta^{\mathrm{T}}(s)\mathcal{N}\zeta(s)]\mathrm{d}s \leqslant 0$.

With some skillful algebraic manipulations [65], it is proven that, if $\hat{\tau}_y$ and $\hat{\tau}_o$ are designed to satisfy

$$(\theta + \wp_4)\wp_1 \leqslant (1-\lambda_o)\sigma_o(1 - \wp_2\wp_4), \quad 1 - \wp_2\wp_4 > 0, \tag{102a}$$

$$\theta\wp_2(1+\wp_5) + \wp_5 + \wp_4\wp_2 \leqslant \lambda_o\sigma_o(1 - \wp_2\wp_4), \tag{102b}$$

$$\theta(\wp_3 + \wp_2\wp_4) + \wp_4 + \wp_4\wp_3 \leqslant \frac{\theta\lambda_y}{\sigma_y}(1 - \wp_2\wp_4), \tag{102c}$$

where

$$\wp_1 = 3\hbar_y(\hat{\tau}_y)\|D_y^{-\frac{1}{2}}P_yL\|^2\|CA\|^2, \ \wp_2 = 3\hbar_y(\hat{\tau}_y)\|D_y^{-\frac{1}{2}}P_yL\|^2\|CBK\|^2, \ \wp_3 = \lambda_yc_y^2/\sigma_y,$$

$$\wp_4 = 3\hbar_o(\hat{\tau}_o)\|D_o^{-\frac{1}{2}}P_oBK\|^2\|L\|^2, \ \wp_5 = 3\hbar_o(\hat{\tau}_o)\|D_o^{-\frac{1}{2}}P_oBK\|^2(\|A+LC\| + \|BK\|)^2 + c_o^2\lambda_o\sigma_o,$$

$$\hbar_y(\hat{\tau}_y) = \int_{t_i^y}^{t_i^y+\hat{\tau}_y} \int_{t_i^y}^{r} \mathrm{d}s\mathrm{d}r,\ \hbar_o(\hat{\tau}_o) = \int_{t_j^o}^{t_j^o+\hat{\tau}_o} \int_{t_j^o}^{r} \mathrm{e}^{2\|BK\|(r-s)}\mathrm{d}s\mathrm{d}r,$$

then the following inequality holds [65]:

$$\begin{bmatrix} 1 & -\wp_2 \\ -\wp_4 & 1 \end{bmatrix} \begin{bmatrix} \int_0^t \|D_y^{-\frac{1}{2}}P_yLe_y(r)\|^2\mathrm{d}r \\ \int_0^t \|D_o^{-\frac{1}{2}}P_oBKe_o(r)\|^2\mathrm{d}r \end{bmatrix} \leqslant \begin{bmatrix} \wp_1 & \wp_3 & \wp_2 \\ 0 & \wp_4 & \wp_5 \end{bmatrix} \begin{bmatrix} \int_0^t \|x_s(r)\|^2\mathrm{d}r \\ \int_0^t \|y(r)\|^2\mathrm{d}r \\ \int_0^t \|x_o(r)\|^2\mathrm{d}r \end{bmatrix} \tag{103}$$

which leads to $\int_0^t [\mathcal{F}(e_y(s), e_o(s)) - \zeta^{\mathrm{T}}(s)\mathcal{N}\zeta(s)]\mathrm{d}s \leqslant 0$.

Step 3: Draw a conclusion. Based the analysis above, the following result is readily obtained.

Theorem 10 ([65, Theorem 3])**.** Suppose that there exist scalars $\theta > 0$, $\mu \in (0,1)$, $\lambda_v \in (0,1)$, $c_v \in (0,1)$, $\sigma_v > 0$, $\hat{\tau}_v > 0$, real matrices $P_v > 0, D_v > 0, Q_v > 0$ with $v \in \{y, o\}$, and real matrices K and L such that (94), (102), and $\mathcal{M} < 0$, where $\mathcal{M}$ is given in (100). Then the system (93) with the modified ETS1 and ETS2 is exponentially stable and Zeno behavior can be excluded.

With the modified ETS1 and ETS2, Theorem 10 provides a sufficient criterion to ensure exponential stability of the closed-loop system (93). This criterion follows an emulation-based approach to design both control gain matrices and event-triggering parameters. Specifically, we first design the control gain K and the observer gain L from (94), leveraging the controllability of (A, B) and the observability of (A, C). Next, we determine the two thresholds λ_y and λ_o based on $\mathcal{M} < 0$. Finally, we design the event-triggering parameters $\hat{\tau}_y$ and $\hat{\tau}_o$ to satisfy the inequalities in (102). It is important to note that these inequalities are closely dependent on both the control gain matrices and the event-triggering parameters, making it challenging to apply the separation principle to the closed-loop system (93) with the modified ETS1 and ETS2.

However, when designing the thresholds λ_y and λ_o based on $\mathcal{M} < 0$, the separation principle can still hold under some circumstances. In fact, an analysis of the matrix $\mathcal{M}$ reveals the following [65].

- There exists a positive constant ℓ_y such that $\mathcal{M} < 0$ for $\lambda_y < \ell_y$. This implies that for a threshold λ_y of ETS1 smaller than ℓ_y, we can independently design the threshold λ_o of ETS2. In other words, fast sampling in the sensor-to-observer channel is sufficient to preserve the separation principle.
- Note that $\mathcal{M} = \mathcal{M}_0 + \lambda_o\sigma_o\mathcal{I}_0$, where

$$\mathcal{M}_0 = \begin{bmatrix} -\mu Q_o + \frac{\theta\lambda_y}{\sigma_y}C^{\mathrm{T}}C & P_oBK \\ \star & -\theta(\sigma_y^{-1}C^{\mathrm{T}}C + \mu Q_y) \end{bmatrix},\ \ \mathcal{I}_0 = \begin{bmatrix} 0 & I \\ \star & I \end{bmatrix}.$$

It has been shown that $\mathcal{M} < 0$ if $\mathcal{M}_0 < 0$ and $\lambda_o < -\lambda_{\min}(\mathcal{M}_0)/(\sigma_o\lambda_{\max}(\mathcal{I}_0))$. Therefore, the separation principle remains valid for fast sampling in the observer-actuator channel under the condition $\mathcal{M}_0 < 0$.

From Theorems 9 and 10, it is clear that applying the separation principle to design event-triggered observer-based output feedback control remains a challenging task, even for linear time-invariant systems. In particular, it is difficult to independently design suitable event-triggered schemes ETS1 and ETS2 that not only ensure the closed-loop system is asymptotically stable but also guarantee positive minimum inter-event times for ETS1 and ETS2.

5 Some other issues related to event-triggered control

5.1 Event-triggered schemes with an ideal execution property

We consider an event-triggered control system described by

$$\dot{x}(t) = Ax(t) + Bu(t),\quad x(t_0) = x_0, \tag{104a}$$

$$u(t) = Kx(t_k),\ t \in [t_k, t_{k+1}), \tag{104b}$$

$$t_{k+1} = \inf\{t > t_k \big| \Im(x) > 0\}, \tag{104c}$$

where $\Im(x)$ is an event-triggering function to determine when an event is triggered. Usually, $\Im(x)$ depends on the measurement error $e(t) = x(t_k) - x(t)$, for instance, $\Im(x) = \Im_1(x) = \|e(t)\| - \sigma\|x(t)\|$ [18]. It is clear that $\Im_1(x)$ is closely related to the norms of $e(t)$ and $x(t)$ rather than themselves. Instead of such an error-based function, in [71, 72], a different event-triggering function is proposed, which reads as

$$\Im_2(x) = V(x(t)) - h(t), \tag{105}$$

where $V(x)$ is a Lyapunov function and $h(t)$ is an admissible Lyapunov level set. The Lyapunov function $V(x)$ is commonly used for stability analysis of the closed-loop system,

$$\dot{x}(t) = (A + BK)x(t) + BKe(t). \tag{106}$$

In an error-based event-triggered scheme, system stability is ensured by requiring that $V(x)$ decreases monotonically along the system trajectory, i.e., $\frac{\mathrm{d}}{\mathrm{d}t}V(x)|_{(106)} < 0$. However, in a Lyapunov-based event-triggered scheme with, i.e., $\Im(x) = \Im_2(x)$, $V(x)$ is not necessarily monotonically decreasing. In fact, $\frac{\mathrm{d}}{\mathrm{d}t}V(x)|_{(106)}$ is allowed to be positive as long as $V(x)$ remains below a predefined threshold $h(t)$ [72]. This concept is later extended in [73] to introduce a less conservative event-triggering condition.

Recently, Lyapunov-based event-triggered schemes have been further developed by introducing a concept of ideal execution [74]. An event-triggering condition $\Im(x) > 0$ is said to have an ideal execution property if for $\forall x(0) \in \mathbb{R}^n$ there exists an exponentially convergent $x(t)$ such that $\Im(x) \leqslant 0$, i.e., no event is generated except at $t = 0$. This ideal execution property implies that no event is triggered if system trajectories are convergent. Therefore, an event-triggering condition with an ideal execution property focuses on detecting when system trajectories begin to diverge, triggering an event immediately upon divergence. With this in mind, an event-triggering function $\Im(x)$ in (104c) is suggested as follows [74]:

$$\Im_3(x) = \frac{\partial V}{\partial x}\Big|_{x=x(t)}\Big[\Phi e(t) + \Omega x(t)\Big], \tag{107}$$

where Φ and Ω are real matrices to be designed. Suppose that $V(x)$ is an ISS Lyapunov function satisfying, for $\forall x, e \in \mathbb{R}^n$,

$$\alpha_{11}\|x\| \leqslant V(x) \leqslant \alpha_{12}\|x\|, \tag{108a}$$

$$\frac{\partial V}{\partial x}\Big[(A + BK)x + BKe\Big] \leqslant -\alpha_{21}V(x) + \alpha_{22}\|e\|, \tag{108b}$$

$$\frac{\partial V}{\partial x}\Big[(A + BK)x + BKe\Big] \geqslant -\alpha_{31}V(x) - \alpha_{32}\|e\|, \tag{108c}$$

where $\alpha_{ij} > 0$ ($i = 1, 2, 3, j = 1, 2$) are constants. Then under the event-triggered scheme (104c) with $\Im(x) = \Im_3(x)$, $\Phi = BK$, and $\Omega = \varepsilon(A + BK)$ ($\varepsilon \in (0, 1)$), the following is proven [74, Theorem 2]:

- The closed-loop system (106) is globally exponentially stable;
- Zeno behavior is excluded;
- The event-triggering condition $\Im_3(x) > 0$ has the ideal execution property.

An event-triggered scheme with the ideal execution property remains inactive while system trajectories are exponentially decaying and becomes active once the Lyapunov function starts increasing. This is the key distinction from schemes such as those in [18, 71, 72]. Alternatively, if we define a dynamic system as

$$\dot{x}(t) = \Phi e(t) + \Omega x(t), \ t \in [t_k, t_{k+1}), \tag{109}$$

then $\Im_3(x)$ can be regarded as the time-derivative of V along the trajectory of the system (109). Consequently, another interpretation of an event-triggered scheme with $\Im(x) = \Im_3(x)$ is that it monitors system trajectory divergence using a dynamic system. In this sense, the event-triggered scheme with $\Im(x) = \Im_3(x)$ can be viewed as a dynamic event-triggered scheme. Such a dynamic event-triggered scheme is different from that in [48], where a dynamic system is designed to monitor the variation of the measurement error norm, rather than system trajectory divergence. On the other hand, it is worth pointing out that under an event-triggered scheme with the ideal execution property, the number of events triggered over the time interval $[t_0, \infty)$ may be finite, meaning that the sampling sequence $\{t_k | k = 1, 2, \ldots\}$ could be a finite sequence.

5.2 Event-triggered control under packet dropouts

In event-triggered control, data packets triggered for transmission may be lost due to limited bandwidth in communication networks [75–77]. Packet dropouts, where an event fails to reach its destination, can significantly impact system performance. Intuitively, techniques such as predictors or estimators can be used to compensate for lost packets by predicting system states, and redundant information or multiple packets can be transmitted to mitigate the effects of dropouts. However, up to date, few effective methods have been developed to address the challenge of event-triggered control with packet dropouts. In the following, we present a brief review of several methods addressing event-triggered control in the presence of packet dropouts.

5.2.1 *Time-delay system method*

In [78], a time-delay system approach is proposed to manage packet dropouts in event-triggered control. This method is based on a uniformly sampled-data system, where the system state is sampled at the sensor side of a networked control system (NCS) with a fixed period $h > 0$. Before transmission, the sampled data are evaluated using an event-triggered scheme. If a predefined event-triggering condition is met, the sampled data are transmitted to the controller, which generates a control signal. This control signal is then immediately sent to the actuator or zero-order-hold (ZOH) to drive the physical plant. With this mechanism, the event-triggered system can be described as

$$\begin{cases} \dot{x}(t) = Ax(t) + B_1 u(t) + B_w w(t),\ x(t_0) = x_0, \\ z(t) = Cx(t) + B_2 u(t), \\ u(t) = Kx(t_k h),\ t \in [t_k h + \tau_{t_k}, t_{k+1} h + \tau_{t_{k+1}}), \end{cases} \tag{110}$$

and the event-triggered scheme is given by

$$\begin{cases} t_{k+1} h = t_k h + \min\{\ell h | e^{\mathrm{T}}(t_k h + \ell h)\Omega e(t_k h + \ell h) > \delta_1 x^{\mathrm{T}}(t_k h)\Omega x(t_k h), \ell = 1, 2, \ldots\}, \\ e(t_k h + \ell h) = x(t_k h + \ell h) - x(t_k h),\ \ell = 0, 1, 2, \ldots, \end{cases} \tag{111}$$

where τ_{t_k} is the transmission delay, and $\Omega > 0, \delta_1 \in [0, 1)$ are triggering parameters. Unlike an input delay approach [79], an artificial delay function $\tau(t)$ is not directly defined as $\tau(t) = t - t_k h$ on the interval $t \in \mathcal{I}_k \triangleq [t_k h + \tau_{t_k}, t_{k+1} h + \tau_{t_{k+1}})$, but defined as $\tau(t) = t - t_k h - rh$ on a small interval $t \in \mathcal{I}_k^r \triangleq [t_k h + rh + \tau_{t_k + rh}, t_k h + rh + h + \tau_{t_k + rh + h})$ with $\mathcal{I}_k = \cup_{r=0}^{q} \mathcal{I}_k^r$, where $q = t_{k+1} - t_k - 1$. Then the event-triggered system (110) is modeled as a time-delay system described by

$$\begin{cases} \dot{x}(t) = Ax(t) + B_1 K[x(t - \tau(t)) - e(t_k h + rh)] + B_w w(t),\ x(t_0) = x_0, \\ z(t) = Cx(t) + B_2 K[x(t - \tau(t)) - e(t_k h + rh)],\ t \in \mathcal{I}_k^r. \end{cases} \tag{112}$$

Let $\delta_2 \leqslant \delta_1 \in [0, 1)$. When the threshold δ_1 in the event-triggered scheme (111) is replaced with δ_2, the triggering instants will change, resulting in a new event-triggered scheme as follows:

$$\begin{cases} s_{k+1} h = s_k h + \min\{\ell h | e^{\mathrm{T}}(s_k h + \ell h)\Omega e(s_k h + \ell h) > \delta_2 x^{\mathrm{T}}(s_k h)\Omega x(s_k h), \ell = 1, 2, \ldots\}, \\ e(s_k h + \ell h) = x(s_k h + \ell h) - x(s_k h),\ \ell = 0, 1, 2, \ldots,\ s_0 = t_0. \end{cases} \tag{113}$$

It is mentioned [78] that the number of events triggered by (113) is greater than that by (111) due to $\delta_2 \leqslant \delta_1$. Thus, an event-triggered scheme with a smaller threshold δ_2 requires more data packets to be transmitted through the communication network, increasing the likelihood of packet dropouts. Based on this observation, when packet dropouts occur, one can opt for a larger threshold δ_1 to trigger events. Suppose that under the event-triggered scheme with δ_1 packet dropouts do not occur. Then under the event-triggered scheme with δ_2, the number of successive pack dropouts is proven to be less than

$$\log_{(1+\sqrt{\delta_2})(1+\varepsilon)} \frac{1 + \sqrt{\delta_1}}{1 + \sqrt{\delta_2}} \ \text{ with } \ \varepsilon = \|Ah\| + \frac{\|hB_1 K\|}{1 - \sqrt{\delta_1}} + \|\epsilon_w h B_w\|, \tag{114}$$

where ϵ_w is a constant such that $\|x(t)\| \leqslant \epsilon_w \|w(t)\|$; see [78] for details. Clearly, this bound depends only on the system matrices, sampling period, and threshold. These results offer an alternative interpretation of event-triggered control in the presence of packet dropouts. However, ensuring no packet loss under the event-triggered scheme with threshold δ_1 remains a significant challenge.

The time-delay system method described above can be applied to event-triggered sampling if the time-delay system model is constructed by dividing the sampling interval into multiple subintervals. Remark that in the time-delay system model (112), the time delay $\tau(t)$ is smaller than the sampling period h, which can be chosen to be relatively short. However, if we set $\tau(t) = t - t_k h,\ t \in \mathcal{I}_k$, the upper bound of $\tau(t)$ could become quite large ($\max\{t_{k+1} - t_k|\ k = 0, 1, \ldots\}$). In such cases, the resulting stability criterion may not be applicable for event-triggered control due to that time-delay systems typically focus on the worst-case scenario of the delay function.

5.2.2 *Hybrid system method*

In [80], a hybrid system method is proposed to address event-triggered control in the presence of packet dropouts. To handle packet dropouts, two configurations, one with and one without an acknowledgment scheme, are considered. With these configurations, two different event-triggered schemes are introduced for dynamic output feedback control, and corresponding hybrid system models are presented for the closed-loop systems. This method is further extended in [81] to a more general case involving two communication channels within the networked systems.

A hybrid system, which exhibits both continuous and discrete dynamic behaviors, can both flow and jump, usually with the following form:

$$\dot{\xi} = F(\xi, w), \quad \text{when } \xi \in \mathcal{C}; \quad \xi^+ \in G(\xi), \quad \text{when } \xi \in \mathcal{D}, \tag{115}$$

where F represents the flow dynamics within the flow set $\mathcal{C}$, and G defines the jump dynamics in the jump set $\mathcal{D}$. Clearly, $\mathcal{C}, \mathcal{D}, F$, and G are four key elements that characterize a hybrid system. For an event-triggered system subject to packet dropouts, Dolk and Heemels [80] provided a method to define $\mathcal{C}, \mathcal{D}, F$, and G.

Consider a networked control system, whose physical plant and dynamic output feedback controller (DOFC) are described, respectively, as

$$\text{Physical plant:} \quad \dot{x}_p(t) = A_p x_p(t) + B_u u(t) + B_w w(t), \qquad y(t) = C_p x_p(t), \tag{116}$$

$$\text{DOFC:} \quad \dot{x}_c(t) = A_c x_c(t) + B_c \tilde{y}(t), \qquad u(t) = C_c x_c(t) + D_c \tilde{y}(t), \tag{117}$$

where $\tilde{y}$ is the most recently received output measurement by the controller. Between updates, $\tilde{y}$ evolves according to $\dot{\tilde{y}}(t) = \tilde{f}(\tilde{y}(t))$, where $\tilde{f}$ is a locally Lipschitz function. In the case of a zero-order-hold, $\tilde{f}$ is identically zero ($\tilde{f} \equiv 0$). An event-triggered scheme is implemented between the physical plant and the controller, operating differently from standard transmission protocols.

• Under transmission control protocols (TCP). Under TCP, the transmitting device knows whether a data packet is transmitted successfully or not. In this situation, the event-triggered scheme is predefined as

$$t_{k+1} = \inf\{t > t_k + \tau_0|\ \eta(t) < 0\}, \tag{118a}$$

$$\begin{cases} \dot{\eta}(t) = \aleph(\zeta(t), \eta(t)), & \text{when } \eta(t) > 0, \\ \eta(t^+) = \eta_0(\zeta(t)), & \text{when } \eta(t) = 0 \text{ and transmission successful}, \\ \eta(t^+) = \eta(t), & \text{when } \eta(t) = 0 \text{ and transmission failed}, \end{cases} \tag{118b}$$

where $\aleph(\cdot,\cdot)$ and $\eta_0(\cdot)$ are two functions to be designed, and $\tau_0 > 0$ is a parameter selected to prevent Zeno behavior. Suppose that the maximum allowable number of successive packet dropouts is $\delta_{\max}$. To model the event-triggered system as a hybrid system, three auxiliary variables are introduced:

(1) $\delta(t) \in \mathcal{I}_\delta \triangleq \{0, 1, 2, \ldots, \delta_{\max}\}$: to track the number of successive packet dropouts;

(2) $\tau(t) \in \mathbb{R}$: to record the time elapsed since the most recent event is triggered;

(3) $\kappa(t) \in \mathbb{N}$: to count the total number of triggered events.

Let $e(t) = \tilde{y}(t) - y(t)$, $x(t) = \mathrm{col}\{x_p(t), x_c(t)\}$, $\xi(t) = \mathrm{col}\{x(t), e(t), \delta(t), \tau(t), \kappa(t), \eta(t)\}$, and $\zeta(t) =$

$\mathrm{col}\{y(t), e(t), \tau(t), \delta(t)\}$. Then,

$$\dot{\xi}(t) = F(\xi(t), w(t)) \triangleq \begin{bmatrix} \left(\begin{smallmatrix}\mathcal{A}_1\\ \mathcal{A}_2\end{smallmatrix}\right)x(t) + \left(\begin{smallmatrix}B_uD_c\\ B_c\end{smallmatrix}\right)e(t) + \left(\begin{smallmatrix}B_w\\ 0\end{smallmatrix}\right)w(t) \\ \tilde{f}(e(t)+y(t)) - C_p\mathcal{A}_1x(t) - C_pB_uD_ce(t) - C_pB_ww(t) \\ 0 \\ 1 \\ 0 \\ \aleph(\zeta(t), \eta(t)) \end{bmatrix}, \tag{119a}$$

$$\xi(t^+) \in G(\xi(t), w(t)) \triangleq \begin{cases} \{G_1(\xi(t), w(t)), G_2(\xi(t), w(t))\}, & \text{when } \delta(t) < \delta_{\max}, \\ \{G_1(\xi(t), w(t))\}, & \text{when } \delta(t) \geqslant \delta_{\max}, \end{cases} \tag{119b}$$

where $\mathcal{A}_1 = [A_p + B_uD_cC_p \;\; B_uC_c]$, $\mathcal{A}_2 = [B_cC_p \;\; A_c]$, and

$$G_1(\xi(t), w(t)) = \mathrm{col}\{x(t), 0, 0, 0, \kappa(t)+1, \eta_0(\zeta(t))\},$$
$$G_2(\xi(t), w(t)) = \mathrm{col}\{x(t), e(t), \delta(t)+1, 0, \kappa(t)+1, \eta(t)\}.$$

The flow set $\mathcal{C}$ and the jump set $\mathcal{D}$ can be given by

$$\mathcal{C} = \{\xi(t) | \tau(t) \leqslant \tau_0 \text{ or } \kappa(t) > \delta_{\max}\},\; \mathcal{D} = \{\xi(t) | \tau(t) \geqslant \tau_0 \text{ and } (\eta(t) = 0 \text{ or } \kappa(t) \leqslant \delta_{\max})\}. \tag{120}$$

Thus, the event-triggered system associated with (116), (117), and (118) is modeled as a hybrid system (115) with (119) and (120). Utilizing hybrid system theory, several asymptotic stability conditions are derived for the resulting event-triggered system, ensuring that its $\mathcal{L}_p$ gain remains below a specified level. Moreover, the event-triggering parameters are carefully designed to achieve this performance.

• Under user diagram protocols (UDP). From (118), the event-triggered scheme relies heavily on information about packet dropouts and sensor measurements between updates. However, under UDP, the transmission protocol lacks an acknowledgement mechanism, meaning that neither packet dropout information nor the sensor measurement $\tilde{y}(t)$ is available. Therefore, the event-triggered scheme (118) should be modified when operating under UDP.

Introduce variables $\tilde{y}_i(t)$ $(i = 1, 2, \ldots, \delta_{\max}+1)$ to track the values of $\tilde{y}(t)$. Let $\tilde{y}_i(t)$ represent the case where there are $i-1$ successive packet dropouts since the most recent successful transmission. The flow dynamics of these variables is defined by $\dot{\tilde{y}}_i(t) = \tilde{f}(\tilde{y}_i(t))$, and the jump dynamics of them is given as $\tilde{y}_1(t^+) = y(t)$ and $\tilde{y}_i(t^+) = \tilde{y}_{i-1}(t)$ $(i = 2, 3, \ldots, \delta_{\max}+1)$. For each $\tilde{y}_i(t)$, introduce a corresponding variable $\eta_i(t)$ in the event-triggered scheme. Then the event-triggered scheme (118) can be modified as

$$t_{k+1} = \inf\{t > t_k + \tau_0 |\; \min\{\eta_i(t) | i = 1, 2, \ldots, \delta_{\max}+1\} < 0\}, \tag{121a}$$

$$\begin{cases} \dot{\eta}_i(t) = \aleph(\tilde{\zeta}_i(t), \eta_i(t)),\; i = 1, 2, \ldots, \delta_{\max}+1, \\ \eta_i(t^+) = \eta_{i-1}(t),\; i = 2, 3, \ldots, \delta_{\max}+1, \\ \eta_1(t^+) = \eta_1^0(t), \end{cases} \tag{121b}$$

where $\tilde{\zeta}_i(t) = \mathrm{col}\{y(t), \tilde{y}_i(t) - y(t), \tau(t), i-1\}$ and $\eta_1^0(t)$ is a design function.

Let $\bar{y}(t) = \mathrm{col}\{\tilde{y}_1(t), \tilde{y}_2(t), \ldots, \tilde{y}_{\delta_{\max}+1}(t)\}$ and $\bar{\eta}(t) = \mathrm{col}\{\eta_1(t), \eta_2(t), \ldots, \eta_{\delta_{\max}+1}(t)\}$. Augment the vector $\xi(t)$ as $\tilde{\xi}(t) = \mathrm{col}\{x(t), e(t), \delta(t), \tau(t), \kappa(t), \eta(t), \bar{y}(t), \bar{\eta}(t)\}$. Similar to the TCP case, a hybrid system for the event-triggered system under UDP can be readily obtained, see [80, Section 6] for details.

From the analysis above, it is evident that the hybrid system method provides an effective framework for modeling event-triggered systems subject to packet dropouts. This model accounts for all relevant information, including the states of the physical plant, controller, event-triggered error dynamics, and instantaneous packet dropouts. By utilizing hybrid system theory, several sufficient conditions for $\mathcal{L}_p$ stability have been derived. However, as seen in (118), the event-triggered scheme is highly dependent on packet dropouts, leading to an implementation challenge. Specifically, it is impossible to 'know' whether a packet will be lost or not before an event is triggered to generate it. Moreover, the method relies on an emulation-based approach, where the control gain should be designed in advance, without reflecting the dynamics of event-triggered operations. Besides, it may be undesirable to introduce a time constant τ_0 in the event-triggered scheme to exclude Zeno behavior.

Event-triggered control in the presence of packet dropouts remains a challenging topic for researchers. Although some promising results have been reported in the literature, effectively handling lost events has yet to be thoroughly addressed. Furthermore, there are no current results on how to handle situations where a data packet generated from an event-triggered scheme is compromised by a false data injection attack.

Beyond the issues of ideal execution and packet dropouts in event-triggered schemes, significant progress has been made in event-triggered control for switched systems [82–87], impulsive systems [88–94], stochastic systems [95–99], and related areas [100–107]. Specifically, for switched systems, the inherent switching behavior introduces additional challenges. In [82], it is assumed that system switchings occur only at triggered instants. In [83], an event-triggered scheme is designed under the assumption that subsystems are perfectly synchronized with their controllers, and such an assumption is relaxed in [85]. In [86], an average dwell time (ADT) switching strategy is proposed, which does not limit the minimum dwell time of each subsystem, thus allowing frequent system switching during an inter-event interval. This approach is then extended to switched affine systems by introducing a time-varying term into the event-triggered scheme [87]. However, in event-triggered switched systems, managing the interplay between inherent switching behavior and event-triggered properties remains a significant theoretical and practical challenge.

To end this section, we briefly highlight an emerging topic: the integration of machine learning (ML) with ETC [108–110]. This integration enhances adaptability, efficiency, and performance in complex control systems but also introduces several challenges due to the inherent trade-offs between computational efficiency, real-time decision-making, and stability guarantees. One key issue is the lack of theoretical stability assurances, as most of the ML models, particularly neural networks, operate as black-box approximators, making it difficult to derive rigorous stability and robustness proofs under event-triggered settings. Another challenge lies in data efficiency and generalization, as training ML models for ETC often requires extensive labeled data, which may not be readily available or representative of diverse operating conditions. Moreover, real-time implementation constraints pose a significant hurdle, as ML-based ETC strategies process data efficiently while adhering to strict triggering conditions, ensuring timely control updates without excessive computational delays. Besides, safety and interpretability concerns arise when using ML for ETC in safety-critical applications, where black-box decisions may be difficult to verify and explain. Finally, adapting ML-driven ETC to networked and distributed systems introduces scalability and communication constraints, requiring decentralized learning approaches that minimize bandwidth usage while maintaining performance. Addressing these challenges is crucial for the practical deployment of ML-enhanced ETC in complex, real-world systems.

6 Conclusion and challenges

ETC provides an efficient solution to balancing control performance with resource constraints in networked systems. By activating control updates only when necessary, ETC can significantly reduce communication and computational loads while ensuring the system's performance. This paper has presented an insightful overview of recent developments in ETC, including data-driven ETC, co-design of control laws and event-triggered schemes, separation principle under event-triggered observer-based output feedback control, ideal execution property of event-triggered schemes, as well as ETC in the presence of packet dropouts. Despite substantial progress that has been made in ETC, challenges still remain to be investigated. Some of them are outlined as follows.

- For systems subject to external disturbances, designing an appropriate event-triggered scheme that avoids Zeno behavior is a challenging task. The commonly used time-regularization method tends to be conservative due to the cautious selection of a time constant. While an accumulated-error-based event-triggered scheme is proposed in [58,111], a key issue remains: the accumulated error does not continuously increase, which requires further investigation to address this limitation.
- More attention should be paid to ETC under packet dropouts. If a data-packet is lost during transmission, the corresponding event is missed, making the event-triggering condition implicit in the Lyapunov stability analysis. Although a hybrid system approach is proposed in [80], limitations remain. Specifically, the event-triggered scheme should be 'aware' of real-time information on packet dropouts,

which is difficult to implement effectively.

• Further research is required to better understand the ideal execution property of event-triggered schemes. A scheme with this property triggers events only when system trajectories begin to diverge, ensuring the minimum number of events necessary to maintain the desired system performance. However, it has been proven in [74] that most of the existing event-triggered schemes do not exhibit the ideal execution property, underscoring the need for ongoing investigation and development.

• While event-triggered control enhances system efficiency by reducing unnecessary data transmission, it also introduces security challenges, particularly in networked systems. Cyberattacks, such as denial-of-service (DoS) or false data injection, can exploit the event-triggering mechanism to disrupt communication or manipulate triggering conditions. Ensuring the security of event-triggered control requires robust designs that account for these potential threats, incorporating mechanisms like attack detection, adaptive control strategies, and resilience to compromised data while maintaining system stability and performance.

• For distributed systems, due to the decentralized nature of decision-making, ETC has always been a hot topic [112–116]. Developing strategies to ensure a minimum inter-event time across multiple agents is critical. Moreover, the joint design of communication protocols and control laws is crucial to optimizing overall system performance. Balancing communication efficiency with control effectiveness requires sophisticated co-design strategies.

• ETC in high-bandwidth and latency-sensitive environments faces several challenges, including uncertain and variable network delays, which can disrupt control performance and stability. Adaptive triggering mechanisms should be designed to handle dynamic network conditions while minimizing unnecessary transmissions. Moreover, real-time decision-making constraints require efficient algorithms that balance computational complexity with responsiveness. Security vulnerabilities, such as adversarial attacks on triggering conditions, pose risks in networked control systems. Addressing these issues is essential for deploying reliable ETC in modern networked control applications.

• Data-driven ETC has been a hot topic in recent years. Although a number of notable results on this topic have been reported, data-driven ETC faces several key challenges. These include the difficulty of designing accurate triggering mechanisms without full system models, ensuring robustness in the presence of unknown disturbances, and managing the trade-off between control performance and resource efficiency. Moreover, integrating data-driven approaches with event-triggering schemes requires overcoming issues such as Zeno behavior, scalability in large systems, and real-time adaptation to dynamic environments. Addressing these challenges is critical to advancing the practical application of data-driven ETC.

Acknowledgements This work was supported in part by National Natural Science Foundation of China (Grant No. 62473221), Natural Science Foundation of Shandong Province, China (Grant No. ZR2024MF006), and Qingdao Natural Science Foundation (Grant No. 24-4-4-zrjj-165-jch).

Open Access funding enabled and organized by CAUL and its Member Institutions.

References

1 Chen Z Y, Han Q-L, Yan Y M, et al. How often should one update control and estimation: review of networked triggering techniques. Sci China Inf Sci, 2020, 63: 150201

2 Behera A K, Bandyopadhyay B, Cucuzzella M, et al. A survey on event-triggered sliding mode control. IEEE J Emerg Sel Top Ind Electron, 2021, 2: 206–217

3 Liu T, Jiang Z P. A small-gain approach to robust event-triggered control of nonlinear systems. IEEE Trans Automat Contr, 2015, 60: 2072–2085

4 Kofman E, Braslavsky J H. Level crossing sampling in feedback stabilization under data-rate constraints. In: Proceedings of the 45th IEEE Conference on Decision and Control, 2006. 4423–4428

5 Mazo M, Tabuada P. On event-triggered and self-triggered control over sensor/actuator networks. In: Proceedings of the 47th IEEE Conference on Decision and Control, 2008. 435–440

6 Heemels W, Johansson K, Tabuada P. An introduction to event-triggered and self-triggered control. In: Proceedings of the 51st IEEE Conference on Decision and Control, 2012. 3270–3285

7 Zeng H B, Zhu Z J, Peng T S, et al. Robust tracking control design for a class of nonlinear networked control systems considering bounded package dropouts and external disturbance. IEEE Trans Fuzzy Syst, 2024, 32: 3608–3617
8 Zhao D, Wang Z, Wei G, et al. A dynamic event-triggered approach to observer-based PID security control subject to deception attacks. Automatica, 2020, 120: 109128
9 Li Y F, Wang X, Sun J, et al. Data-driven consensus control of fully distributed event-triggered multi-agent systems. Sci China Inf Sci, 2023, 66: 152202
10 Chang Z Z, Song W H, Wang J J, et al. Fully distributed event-triggered affine formation maneuver control over directed graphs. Sci China Inf Sci, 2023, 66: 164201
11 Yang H, Peng C, Cao Z, et al. A novel semantic-based multi-packet parallel transmission scheme for networked control systems. Automatica, 2025, 174: 112120
12 Ding D R, Han Q-L, Ge X H, et al. Privacy-preserving filtering, control and optimization for industrial cyber-physical systems. Sci China Inf Sci, 2025, 68: 141201
13 Ge X H, Han Q-L, Zhang X-M, et al. Distributed coordination control of multi-agent systems under intermittent sampling and communication: a comprehensive survey. Sci China Inf Sci, 2025, 68: 151201
14 Zhang D, Han Q-L, Jia X. Network-based output tracking control for a class of T-S fuzzy systems that can not be stabilized by nondelayed output feedback controllers. IEEE Trans Cybern, 2015, 45: 1511–1524
15 Kopetz H. Event-triggered versus time-triggered real-time systems. In: Operating Systems of the 90s and Beyond. Berlin: Springer, 1991
16 Kopetz H. Should responsive systems be event-triggered or time-triggered? IEICE Trans Inform Syst Jpn, 1993, E76-D: 1325–1332
17 Åström K J, Bernhardsson B. Comparison of periodic and event based sampling for first-order stochastic systems. IFAC Proc Volumes, 1999, 32: 5006–5011
18 Tabuada P. Event-triggered real-time scheduling of stabilizing control tasks. IEEE Trans Automat Contr, 2007, 52: 1680–1685
19 Xiao H C, Ding D R, Dong H L, et al. Adaptive event-triggered state estimation for large-scale systems subject to deception attacks. Sci China Inf Sci, 2022, 65: 122207
20 Wang X, Sun J, Deng F, et al. Event-triggered consensus control of heterogeneous multi-agent systems: model- and data-based approaches. Sci China Inf Sci, 2023, 66: 192201
21 Sun Q, Chen J C, Shi Y. Event-triggered robust MPC of nonlinear cyber-physical systems against DoS attacks. Sci China Inf Sci, 2022, 65: 110202
22 Yu H, Hao F. Input-to-state stability of integral-based event-triggered control for linear plants. Automatica, 2017, 85: 248–255
23 Shi Y, Hu Q, Shao X, et al. Adaptive neural coordinated control for multiple Euler-Lagrange systems with periodic event-triggered sampling. IEEE Trans Neural Netw Learn Syst, 2023, 34: 8791–8801
24 Tang Y, Jin X, Shi Y, et al. Event-triggered attitude synchronization of multiple rigid body systems with velocity-free measurements. Automatica, 2022, 143: 110460
25 Wang X H, Wang Z, Xia J W, et al. Adaptive event-trigger-based sampled-data stabilization of complex-valued neural networks: a real and complex LMI approach. Sci China Inf Sci, 2023, 66: 149203
26 Wang X, Sun J, Wang G, et al. Data-driven control of distributed event-triggered network systems. IEEE CAA J Autom Sin, 2023, 10: 351–364
27 Chai J, Lu Q, Tao X, et al. Dynamic event-triggered fixed-time consensus control and its applications to magnetic map construction. IEEE CAA J Autom Sin, 2023, 10: 2000–2013
28 Wang S, Wang Z, Dong H, et al. Dynamic event-triggered quadratic nonfragile filtering for non-Gaussian systems: tackling multiplicative noises and missing measurements. IEEE CAA J Autom Sin, 2024, 11: 1127–1138
29 Xie X, Liu Y, Li Q. Neural network-based adaptive event-triggered control for cyberphysical systems under resource constraints and hybrid cyberattacks. Automatica, 2023, 152: 110977
30 Du D, Qi B, Fei M, et al. Quantized control of distributed event-triggered networked control systems with hybrid wired C wireless networks communication constraints. Inf Sci, 2017, 380: 74–91
31 Zhou T, Zuo Z, Wang Y. Active event-triggered control for nonlinear networked control systems with communication constraints. IEEE Trans Cybern, 2021, 51: 2409–2418
32 Zhang J Y, Ma Y C. Parallel event-triggered dynamic output feedback control for nonlinear networked systems with randomly occurring multiple communication delays. ISA Trans, 2024, 151: 1–11
33 Li Z, Wang X, Xi L, et al. Event-triggered output-feedback control for high-order uncertain nonlinear multiagent systems subject to denial-of-service attacks. IEEE Internet Things J, 2024, 11: 23661–23672
34 Cao Z, Fu J. Dynamic output feedback control of switched systems: a dynamic event-triggered sampling control scheme. Syst Control Lett, 2024, 186: 105773
35 Borgers D P, Heemels W P M H. Event-separation properties of event-triggered control systems. IEEE Trans Automat Contr, 2014, 59: 2644–2656
36 Peng C, Li F. A survey on recent advances in event-triggered communication and control. Inf Sci, 2018, 457-458: 113–125
37 Zhang X M, Han Q-L, Ge X, et al. Networked control systems: a survey of trends and techniques. IEEE CAA J Autom Sin, 2020, 7: 1–17
38 Ge X, Han Q-L, Zhang X M, et al. Distributed event-triggered estimation over sensor networks: a survey. IEEE Trans Cybern, 2020, 50: 1306–1320

39 Zhang P, Liu T, Chen J, et al. Recent developments in event-triggered control of nonlinear systems: an overview. Unmanned Syst, 2023, 11: 27–56

40 Zhang X M, Han Q-L, Ge X, et al. Sampled-data control systems with non-uniform sampling: a survey of methods and trends. Annu Rev Control, 2023, 55: 70–91

41 Yue D, Tian E, Han Q-L. A delay system method for designing event-triggered controllers of networked control systems. IEEE Trans Automat Contr, 2013, 58: 475–481

42 Peng C, Han Q-L. A novel event-triggered transmission scheme and $\mathcal{L}_2$ control co-design for sampled-data control systems. IEEE Trans Automat Contr, 2013, 58: 2620–2626

43 Zhang X M, Han Q-L, Zhang B L. An overview and deep investigation on sampled-data-based event-triggered control and filtering for networked systems. IEEE Trans Ind Inf, 2017, 13: 4–16

44 Liu W, Sun J, Wang G, et al. Data-driven self-triggered control via trajectory prediction. IEEE Trans Automat Contr, 2023, 68: 6951–6958

45 Wang X, Berberich J, Sun J, et al. Model-based and data-driven control of event- and self-triggered discrete-time linear systems. IEEE Trans Cybern, 2023, 53: 6066–6079

46 de Persis C, Postoyan R, Tesi P. Event-triggered control from data. IEEE Trans Automat Contr, 2024, 69: 3780–3795

47 Lopez V, Müller M. On a continuous-time version of Willems' lemma. In: Proceedings of IEEE 61st Conference on Decision and Control (CDC), Austin, 2022. 2759–2764

48 Girard A. Dynamic triggering mechanisms for event-triggered control. IEEE Trans Automat Contr, 2015, 60: 1992–1997

49 Digge V, Pasumarthy R. Data-driven event-triggered control for discrete-time LTI systems. In: Proceedings of European Control Conference (ECC), London, 2022. 1355–1360

50 Qi W L, Liu K Z, Wang R, et al. Data-driven $\mathcal{L}_2$-stability analysis for dynamic event-triggered networked control systems: a hybrid system approach. IEEE Trans Ind Electron, 2023, 70: 6151–6158

51 de Persis C, Tesi P. Formulas for data-driven control: stabilization, optimality, and robustness. IEEE Trans Automat Contr, 2020, 65: 909–924

52 Willems J C, Rapisarda P, Markovsky I, et al. A note on persistency of excitation. Syst Control Lett, 2005, 54: 325–329

53 Hou Z S, Wang Z. From model-based control to data-driven control: survey, classification and perspective. Inf Sci, 2013, 235: 3–35

54 Seuret A. A novel stability analysis of linear systems under asynchronous samplings. Automatica, 2012, 48: 177–182

55 Zhang X M, Wu M, She J H, et al. Delay-dependent stabilization of linear systems with time-varying state and input delays. Automatica, 2005, 41: 1405–1412

56 Zeng H B, Teo K L, He Y. A new looped-functional for stability analysis of sampled-data systems. Automatica, 2017, 82: 328–331

57 Ghodrat M, Marquez H J. On the event-triggered controller design. IEEE Trans Automat Contr, 2020, 65: 4122–4137

58 Zhang X-M, Han Q-L, Zhang B-L, et al. Accumulated-state-error-based event-triggered sampling scheme and its application to H_∞ control of sampled-data systems. Sci China Inf Sci, 2024, 67: 162206

59 Zhang X, Han Q. Event-triggered dynamic output feedback control for networked control systems. IET Control Theor & Appl, 2014, 8: 226–234

60 Zhang X M, Han Q-L. A decentralized event-triggered dissipative control scheme for systems with multiple sensors to sample the system outputs. IEEE Trans Cybern, 2016, 46: 2745–2757

61 Dolk V S, Borgers D P, Heemels W P M H. Output-based and decentralized dynamic event-triggered control with guaranteed $\mathcal{L}_p$-gain performance and zeno-freeness. IEEE Trans Automat Contr, 2017, 62: 34–49

62 Abdelrahim M, Postoyan R, Daafouz J, et al. Robust event-triggered output feedback controllers for nonlinear systems. Automatica, 2017, 75: 96–108

63 Abdelrahim M, Postoyan R, Daafouz J, et al. Co-design of output feedback laws and event-triggering conditions for the L_2-stabilization of linear systems. Automatica, 2018, 87: 337–344

64 Ban J, Seo M, Goh T, et al. Improved co-design of event-triggered dynamic output feedback controllers for linear systems. Automatica, 2020, 111: 108600

65 Ghodrat M, Marquez H J. A separation principle for linear event-triggered output feedback systems. IEEE Trans Automat Contr, 2022, 67: 1498–1505

66 Durand S, Torres L, Guerrero-Castellanos J F. Event-triggered observer-based output-feedback stabilization of linear system with communication delays in the measurements. In: Proceedings of the 13th European Control Conference, 2014, 666–671

67 Garcia E, Antsaklis P. Event-triggered output feedback stabilization of networked systems with external disturbance. In: Proceedings of the 53rd IEEE Conference on Decision and Control, 2014. 3566–3571

68 Etienne L, Gennaro S D, Barbot J P. Event triggered observer-based control for linear systems with time varying uncertainties. In: Proceedings of the American Control Conference, 2015. 1531–1536

69 Tanwani A, Prieur C, Fiacchini M. Observer-based feedback stabilization of linear systems with event-triggered sampling and dynamic quantization. Syst Control Lett, 2016, 94: 46–56

70 Tarbouriech S, Seuret A, da Silva J M G, et al. Observer-based event-triggered control co-design for linear systems. IET Control Theor & Appl, 2016, 10: 2466–2473

71 Wang X, Lemmon M. Event design in event-triggered feedback control systems. In: Proceedings of the 47th IEEE Conference on Decision and Control, 2008. 2105–2110

72 Wang X, Lemmon M. On event design in event-triggered feedback systems. Automatica, 2011, 47: 2319–2322

73 Durand S, Marchand N, Castellanos J F G. Simple Lyapunov sampling for event-driven control. In: Proceedings of the 18th

IFAC World Congress, 2011. 8724–8730
74 Ghodrat M, Marquez H J. A new Lyapunov-based event-triggered control of linear systems. IEEE Trans Automat Contr, 2023, 68: 2599–2606
75 Zhang X M, Han Q-L, Ge X. A novel approach to H_∞ performance analysis of discrete-time networked systems subject to network-induced delays and malicious packet dropouts. Automatica, 2022, 136: 110010
76 Zhang D, Han Q-L, Zhang X M. Network-based modeling and proportional-integral control for direct-drive-wheel systems in wireless network environments. IEEE Trans Cybern, 2020, 50: 2462–2474
77 Hu Z, Ren H, Deng F, et al. Stabilization of sampled-data systems with noisy sampling intervals and packet dropouts via a discrete-time approach. IEEE Trans Automat Contr, 2022, 67: 3204–3211
78 Peng C, Yang T C. Event-triggered communication and H_∞ control co-design for networked control systems. Automatica, 2013, 49: 1326–1332
79 Fridman E, Seuret A, Richard J P. Robust sampled-data stabilization of linear systems: an input delay approach. Automatica, 2004, 40: 1441–1446
80 Dolk V, Heemels M. Event-triggered control systems under packet losses. Automatica, 2017, 80: 143–155
81 Zhu X L, Zhang X, Wei J, et al. Output-based dynamic event-triggered control for networked control systems with delays and packet losses without acknowledgements. IEEE Trans Automat Contr, 2023, 68: 7120–7135
82 Xiang W, T. Johnson T. Event-triggered control for continuous-time switched linear systems. IET Control Theor & Appl, 2017, 11: 1694–1703
83 Li T F, Fu J. Event-triggered control of switched linear systems. J Franklin Institute, 2017, 354: 6451–6462
84 Qi Y, Cao M. Finite-time boundedness and stabilisation of switched linear systems using event-triggered controllers. IET Control Theor & Appl, 2017, 11: 3240–3248
85 Li T F, Fu J, Deng F, et al. Stabilization of switched linear neutral systems: an event-triggered sampling control scheme. IEEE Trans Automat Contr, 2018, 63: 3537–3544
86 Fei Z, Guan C, Zhao X. Event-triggered dynamic output feedback control for switched systems with frequent asynchronism. IEEE Trans Automat Contr, 2020, 65: 3120–3127
87 Li Z, Zhao J. A zeno-free event-triggered control strategy for asymptotic stabilization of switched affine systems. IEEE Trans Automat Contr, 2022, 67: 5509–5516
88 Liu B, Hill D J, Sun Z. Stabilisation to input-to-state stability for continuous-time dynamical systems via event-triggered impulsive control with three levels of events. IET Control Theor & Appl, 2018, 12: 1167–1179
89 Li X, Yang X, Cao J. Event-triggered impulsive control for nonlinear delay systems. Automatica, 2020, 117: 108981
90 Li X, Li P. Input-to-state stability of nonlinear systems: event-triggered impulsive control. IEEE Trans Automat Contr, 2022, 67: 1460–1465
91 Li X, Wang M. Stability for nonlinear delay systems: self-triggered impulsive control. Automatica, 2024, 160: 111469
92 Tan X, Cao J, Li X. Consensus of leader-following multiagent systems: a distributed event-triggered impulsive control strategy. IEEE Trans Cybern, 2019, 49: 792–801
93 Zhou Y, Zeng Z. Event-triggered impulsive control on quasi-synchronization of memristive neural networks with time-varying delays. Neural Netws, 2019, 110: 55–65
94 Yao M, Wei G. Dynamic event-triggered control of continuous-time systems with random impulses. IEEE CAA J Autom Sin, 2023, 10: 2292–2299
95 Quevedo D E, Gupta V, Ma W J, et al. Stochastic stability of event-triggered anytime control. IEEE Trans Automat Contr, 2014, 59: 3373–3379
96 Wang Y, Zheng W X, Zhang H. Dynamic event-based control of nonlinear stochastic systems. IEEE Trans Automat Contr, 2017, 62: 6544–6551
97 Gao Y F, Sun X M, Wen C, et al. Event-triggered control for stochastic nonlinear systems. Automatica, 2018, 95: 534–538
98 Zhu Q. Stabilization of stochastic nonlinear delay systems with exogenous disturbances and the event-triggered feedback control. IEEE Trans Automat Contr, 2019, 64: 3764–3771
99 Zhu Q. Event-triggered sampling problem for exponential stability of stochastic nonlinear delay systems driven by Lévy processes. IEEE Trans Automat Contr, 2025, 70: 1176–1183
100 Ji C, Zhang Z, Ge S S. Adaptive event-triggered output feedback control for uncertain parabolic PDEs. Automatica, 2025, 171: 111917
101 Ding L, Ye M, Yue D. Communication-efficient distributed Nash equilibrium seeking under switching topologies: a decentralized gradient-based event-triggered scheme. Automatica, 2024, 167: 111738
102 Ji R, Ge S S, Zhao K. Coded event-triggered control for nonlinear systems. Automatica, 2024, 167: 111753
103 Sabouni E, Cassandras C G, Xiao W, et al. Optimal control of connected automated vehicles with event/self-triggered control barrier functions. Automatica, 2024, 162: 111530
104 Kang W, Zhang J, Wang J M. Disturbance rejection approaches of Korteweg-de Vries-Burgers equation under event-triggering mechanism. Automatica, 2024, 169: 111844
105 Li Y, Wu Y, He S, et al. Leader-following consensus tracking of autonomous unmanned systems with fixed/switching topologies: an event-triggered approach. Int J Syst Sci, 2020, 51: 2441–2455
106 Jiang W, Luo M, Cheng J, et al. Adaptive event-triggered lateral control for autonomous vehicle system under stochastic-sampling subject to dynamic quantization. Intl J Robust Nonlinear, 2024, 34: 11819–11844
107 Ponnarasi L, Pankajavalli P B, Lim Y, et al. Optimization-based event-triggered state estimation algorithm for IoT-based wind turbine systems. IEEE Internet Things J, 2024, 11: 9645–9655

108 Ghosh S, Aquino B, Gupta V. EventGraD: event-triggered communication in parallel machine learning. Neurocomputing, 2022, 483: 474–487

109 Cai X, Shi K, Sun Y, et al. Intelligent event-triggered control supervised by mini-batch machine learning and data compression mechanism for T-S fuzzy NCSs under DoS attacks. IEEE Trans Fuzzy Syst, 2024, 32: 804–815

110 Sedghi L, Ijaz Z, Noor-A-Rahim M, et al. Machine learning in event-triggered control: recent advances and open issues. IEEE Access, 2022, 10: 74671–74690

111 Zhang X M, Han Q-L, Ge X, et al. Accumulative-error-based event-triggered control for discrete-time linear systems: a discrete-time looped functional method. IEEE CAA J Autom Sin, 2025, 12: 683–693

112 Selivanov A, Fridman E. Distributed event-triggered control of diffusion semilinear PDEs. Automatica, 2016, 68: 344–351

113 Yan H, Zhang H, Yang F, et al. Event-triggered asynchronous guaranteed cost control for Markov jump discrete-time neural networks with distributed delay and channel fading. IEEE Trans Neural Netw Learn Syst, 2018, 29: 3588–3598

114 Hu W, Yang C, Huang T, et al. A distributed dynamic event-triggered control approach to consensus of linear multiagent systems with directed networks. IEEE Trans Cybern, 2020, 50: 869–874

115 Ge X, Han Q-L, Ding L, et al. Dynamic event-triggered distributed coordination control and its applications: a survey of trends and techniques. IEEE Trans Syst Man Cybern Syst, 2020, 50: 3112–3125

116 Dimarogonas D V, Frazzoli E, Johansson K H. Distributed event-triggered control for multi-agent systems. IEEE Trans Automat Contr, 2012, 57: 1291–1297